University of Tennessee, Knoxville
Trace: Tennessee Research and Creative Exchange

Masters Theses Graduate School

12-2014

Adomian Decomposition of the Flowfield in a Simulated Rocket Motor

Jeisson Juliany Parra
University of Tennessee - Knoxville, jparra@vols.utk.edu

To the Graduate Council:

I am submitting herewith a thesis written by Jeisson Juliany Parra entitled "Adomian Decomposition of the Flowfield in a Simulated Rocket Motor." I have examined the final electronic copy of this thesis for form and content and recommend that it be accepted in partial fulfillment of the requirements for the degree of Master of Science, with a major in Aerospace Engineering.

Joseph Majdalani, Major Professor

We have read this thesis and recommend its acceptance:

Basil N. Antar, Christian G. Parigger

Accepted for the Council:
Carolyn R. Hodges

Vice Provost and Dean of the Graduate School

(Original signatures are on file with official student records.)

Adomian Decomposition of the Flowfield

in a Simulated Rocket Motor

A Thesis Presented for the

Master of Science

Degree

The University of Tennessee, Knoxville

Jeisson Juliany Parra

December 2014

Dedication

I dedicate my thesis to my loving family. Your support and encouragement provided me with the motivation to see this work to its completion. Thank you for everything.

Acknowledgments

I would like to thank Dr. Joseph Majdalani for his assistance, his motivation, his patience, and his mentorship that were essential to the completion of this work. I would also like to thank the faculty and staff at the University of Tennessee Space Institute and the University of Tennessee in Knoxville, particularly my thesis committee members, Dr. Basil Antar and Dr. Christian Parigger, for taking the time to assist me in completing the requirements for this degree

Abstract

The work presents an analytic, approximate solution to an internal flowfield for a solid rocket motor. The flowfield is modeled as a wall-normal injection or suction in a symmetric porous channel with laterally expanding or contracting walls. From the effective speeds that gases are ejected into the combustion chamber of typical rocket motors, the flowfield is modeled to be incompressible. Since the flame zone occurs in a very thin space above the propellant grain surface, it will be disregarded. Assuming linearly varying axial velocity and uniform expansion (or contraction), the Navier-Stokes equations will be reduced into a single nonlinear equation that can be solved asymptotically. The Adomian Decomposition Method is used to solve this problem. Its systematic approach to solving differential equations makes it ideally suited for the present application. With this method one can recover an exact solution for problems that allow an analytic treatment, it can also be used to arrive at approximate solutions for problems that cannot be solved exactly. The governing equation that describes the bulk fluid motion within the rocket chamber and the solution provided here will take into account the viscosity, wall regression, and wall permeability.

Table of Contents

List of Figures

Nomenclature

$\dot{a}$	=	wall regression/expansion speed
a	=	channel half-spacing, radius of a porous cylinder
A	=	injection coefficient, constant of proportionality
F	=	Berman's characteristic mean flow function
p	=	pressure
R	=	Reynolds number, crossflow Reynolds number, sidewall injection Reynolds number
R_b	=	blowing Reynolds number
Re_{inj}	=	wall injection Reynolds number
t	=	time
u	=	velocity component, x-direction
v	=	velocity component, y-direction
V_w	=	normal injection speed, absolute speed of injection, crossflow injection speed at the wall
V_b	=	blowing speed relative to the moving wall
$\overline{x}$	=	axial distance from the headwall

Greek

~	=	wall expansion ratio, secondary perturbation parameter
£	=	small parameter
¦	=	$\frac{y}{a}, \frac{1}{2}r^2$
¸	=	flow vorticity, $-\nabla^2$·
·	=	streamfunction
«	=	dynamic viscosity
¬	=	kinematic viscosity, «/°

°	=	dimensional density

Superscripts

′	=	first derivative
″	=	second derivative
(3) or ‴	=	third-order derivative
(4) or ⁗	=	fourth-order derivative

Chapter 1

Introduction

The analysis of wall-injected ducted flows remains a recurrent topic in the fluid dynamics and propulsion communities, owing in large part to the wealth of applications in which wall-normal injection is present. Depending on the application at hand, porous walls can be used to simulate different types of surface mechanisms. These include membrane separation, sweat cooling, boundary layer control, surface transpiration, phase change (e.g., sublimation of solidified carbon dioxide), paper manufacturing, irrigation, and, most notably in propulsive applications, grain regression and propellant burning. Similar events occur in a number of interesting models of biologically inspired flows, peristaltic motion, pulmonary respiration, biocirculation, flow filtration, chemical dispensing, and reverse osmosis.

The initiation of studies into porous channel flows is well attributed to work by Berman [1]. In this pioneering article, Berman investigates the mechanisms associated with the industrial separation of U_{235} from U_{238} through a process known as gas diffusion. Consequently, recognizing that the wall-normal velocity in a porous duct must remain independent of the axial distance from the headwall, Berman is able to reduce the Navier-Stokes equations into a single, nonlinear, fourth-order ODE that is known as Berman's equation. His resulting ODE can be expressed both in Cartesian and cylindrical coordinates, depending on whether the problem is planar (2D) or axisymmetric (polar cylindrical, with no variations in the tangential direction). Berman's ordinary differential equation is subject to four fundamental boundary conditions and a crossflow Reynolds number, R. In this work, the small injection case is investigated, thus only small values of R will be considered. This Reynolds number is also referred to as the wall injection Reynolds number, Re_{inj}, especially in the propulsion community [2]. It is based on the normal injection speed, V_w, and the channel half-spacing a. In the axisymmetric geometry, a is taken to be the radius of the porous cylinder.

For small values of R, Berman obtains a regularly perturbed asymptotic expansion to the problem in question. Several related investigations later follow, and these are based on either analytical or computational techniques. Analytical approaches that are used in this context are diverse. They rely on methods such as integral analysis, method of averages, least-squares, power-series solutions, boundary layer theory, matched-asymptotic expansions, and multiple scales theories. Examples abound, and the interested reader may consult with the highly cited papers by Taylor [3], Yuan [4] and Terrill [5] (for large sidewall injection), Sellars [6] and Terrill [7] (for large sidewall suction), Proudman [8] and Shrestha and Terrill [9] (for large R and both symmetric and asymmetric sidewall injection), Morduchow [10] and White, Barfield and Goglia [11] (for arbitrary levels of sidewall injection). Investigations of asymmetric flow motion and temporal instability have also been performed by Cox [12], King and Cox [13], Zaturska, Drazin and Banks [14], Taylor, Banks, Zaturska and Drazin [15] and Watson, Banks, Zaturska and Drazin [16,17]. In what concerns the large suction case, some of the most elegant asymptotic treatment may be found in Cox and King [18], MacGillivray and Lu [19], and Lu [20].

The spatial instability of Berman-related solutions constitutes a separate topic that has opened up new lines of research inquiry. Investigations of this sort may be traced back to work by Varapaev and Yagodkin [21], Raithby and Knudsen [22], Hocking [23], Sviridenkov and Yagodkin [24], Brady [25], Durlofsky and Brady [26], and others. On this particular subject, the characterization and identification of multiple solutions that can arise over different ranges of the Reynolds number, R, are reported in articles by Robinson [27], Skalak and Wang [28], Shih [29], Hastings, Lu and MacGillivray [30], and Lu, MacGillivray and Hastings [31]. Under wall-injection conditions, only unique and stable symmetrical solutions are shown to exist for the entire range of the injection Reynolds number. This result is first reported by Skalak and Wang [28] and later confirmed using mathematical proof by Shih [29] and Hastings, Lu and MacGillivray [30]. For suction-induced motion in a porous channel, it is shown that one of the symmetric solutions can turn unstable in the presence of asymmetric disturbances. Subsequently, it can bifurcate into a pair of asymmetric solutions in the suction range corresponding to $-\infty < R < -6.0014$.

For a comprehensive survey of all possible configurations that correspond to suction-induced motions, the articles by Zaturska, Drazin and Banks [14], and Cox and King [18] may be referenced. Other useful studies include those by Cox [12], King and Cox [13], and Taylor, Banks, Zaturska and Drazin [15].

Besides theoretical modeling, several numerical and experimental studies have been carried out in an effort to better understand the character of the flow in porous channels. Though the list may be too long to enumerate, one may begin with Taylor [3], whose work associated with flow through thin porous sheets led to the first analytical solution for the large wall-injection problem. His solutions later proved to be accurate not only for the porous channel configuration, but also for the porous tube and wedge geometries. Other studies include those by Varapaev and Yagodkin [21], Raithby and Knudsen [22], Sviridenkov and Yagodkin [24], Casalis, Avalon and Pineau [32], Saad and Majdalani [33], and Kurdyumov [34]. In short, all of these studies concur that in the case of wall-normal injection, the analytical approximations obtained by Taylor [3], Yuan [4], and Terrill [5] will develop quite rapidly into a self-similar form inside a porous channel. In the case of suction, however, more than one solution is reported, including the simple approximation derived by Sellars [6] and later confirmed by Terrill [7]. The analytical model for the large injection case has been frequently employed to model the internal flowfield in a solid rocket motor.

Despite the high temperature within solid rocket motors, Chu, Yang and Majdalani [35] and Vyas, Majdalani and Yang [36] have demonstrated that the majority of chemical reactions due to burning propellant remain confined to a thin layer above the solid propellant grain. The thickness of this layer in most practical applications does not exceed 5% of the chamber diameter. Calculating the blowing speed along the edge of this layer enables us to treat the gaseous motion within the chamber as non-reactive. The resulting bulk motion may be captured by the streamlines depicted in Fig. 1, where the wall-normal injection along the simulated propellant grain is illustrated.

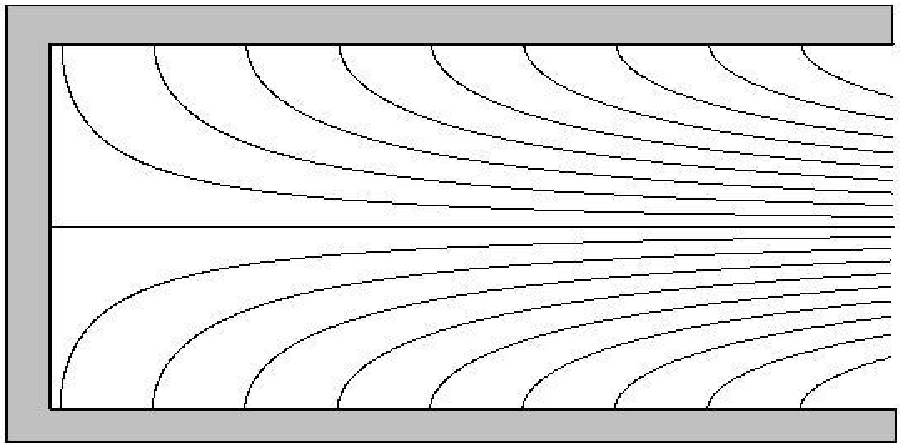

Figure 1. Streamlines associated with the bulk gaseous motion in solid rocket motors.

In actual motor firings, the internal volume of the combustion chamber expands radially outwardly as time passes in view of grain regression. In typical motors, gases are ejected into the chamber at effective speeds that fall in the range of 2-7 m/s. The average mean flow Mach number inside the chamber up to and excluding the nozzle entrance region does not usually exceed a value of 0.3. By virtue of the thin flame zone in which chemical reactions are confined, the flame zone may be disregarded, and blowing or injection may be taken to occur along the propellant surface itself. The resulting flowfield may be treated as an incompressible fluid in a porous channel with laterally expanding walls.

The purpose of this thesis is to extend previous investigations by presenting a new analytical solution for small injection in a porous channel with expanding or contracting walls. To be realistic, only symmetric configurations will be considered.

A main objective of this work is to leverage the use of the Adomian Decomposition to obtain new approximations for this problem. Another objective is to overcome deficiencies in available solutions that do not account for viscosity, wall regression, wall permeability, or some combination of these fundamental flow features. In the present work, all of these ingredients will be incorporated.

In modeling the internal flowfield in solid rocket motors, most previous studies have discounted the effects of viscous shear and grain burnback. The use of the inviscid Taylor profile became common, although studies by Apte and Yang [37], Lee and Beddini [38,39], and Majdalani [40] have confirmed the importance of retaining viscous dissipation terms due to their appreciable contributions to the attenuation or growth of vortico-acoustic waves. Viscosity does not only alter the bulk flow motion, but it can also influence the motor stability formulation in which the proper assessment of vortical energy is paramount. Furthermore, the inclusion of viscous effects in the base flow description leads to a consistently viscous vortico-acoustic solution in which fluid resistance is equally retained in both mean and unsteady velocities. This enables us to refine the vortico-acoustic solutions presented recently by Majdalani [40] or Majdalani and Roh [41].

Along similar lines, retention of wall regression stands to improve our accuracy in modeling energetic and fast burning propellants developed for high-acceleration vehicles [42,43]. It also increases our repertoire of engineering approximations for modeling the ablating surfaces of re-entry vehicles that depend on transpiration cooling [44]. It may also be used to mimic the sublimation process of dry ice (or solid CO2), a phase change mechanism that has been recurrently used to simulate the burnback of solid propellant grains [45-47].

Finally, the repetitive sequence of expansions and contractions that are undertaken by porous channel walls can be used to model the peristaltic motion associated with fluid absorption [48,49]. The analytical framework to be developed here can therefore provide guidance to physiologists who are concerned with the modeling of fluid seepage and filtration processes [50-52] that often take place between parallel flat membranes. The framework will therefore consider 'slit flows' that arise in narrow passages with compliant membranes as part of the forthcoming formulation.

To derive the governing equation, we blend the tools employed by Berman [1], Yuan [4], Sellars [6], Terrill [7], and Goto and Uchida [49]. Assuming linearly varying axial velocity (or streamfunction) and uniform expansion (or contraction), the Navier-Stokes equations will be reduced into a single nonlinear equation that can be solved asymptotically. Depending on whether injection or suction is present, different analytical procedures will be implemented to arrive at closed-form approximations for Berman's characteristic mean flow function, F. If desired, based on F, the magnitude of the velocity, pressure and shear stresses can be deduced and used to characterize the corresponding flow motion.

Chapter 2

Geometry and Governing Equations

In this chapter, the geometry associated with the simulated porous channel will be defined. Furthermore, the governing equations for the viscous and incompressible motion will be reconstructed to illuminate the origin of the equation that will be used in subsequent analysis.

A. Geometry

The geometry under consideration is shown in Figure 2. The flow to be studied evolves inside a 2D porous channel that is bounded by porous walls at $\bar{y} = \pm a$, where $\bar{x}$ denotes the axial distance from the headwall. The porous walls of the channel undergo uniform expansion or contraction in the transverse direction. Through the two opposing walls of the chamber, a viscous fluid is uniformly injected or withdrawn at a spatially uniform speed, V_w. It should be noted that although the flow in cylindrical tubes with circular cross-sections are more common than planar flows; the latter are of equal academic importance. Not only are they more straightforward to describe, they also develop in porous channels and low aspect ratio enclosures that are often modeled as 'slit' flows, or flows between parallel plates. In this particular configuration, the flow field is induced by wall-normal suction or injection that is uniformly distributed along the sidewall. The use of Cartesian coordinates to describe the motion in planar geometry leads to a simplification in the desired solution that can yet capture the essential features of the flow.

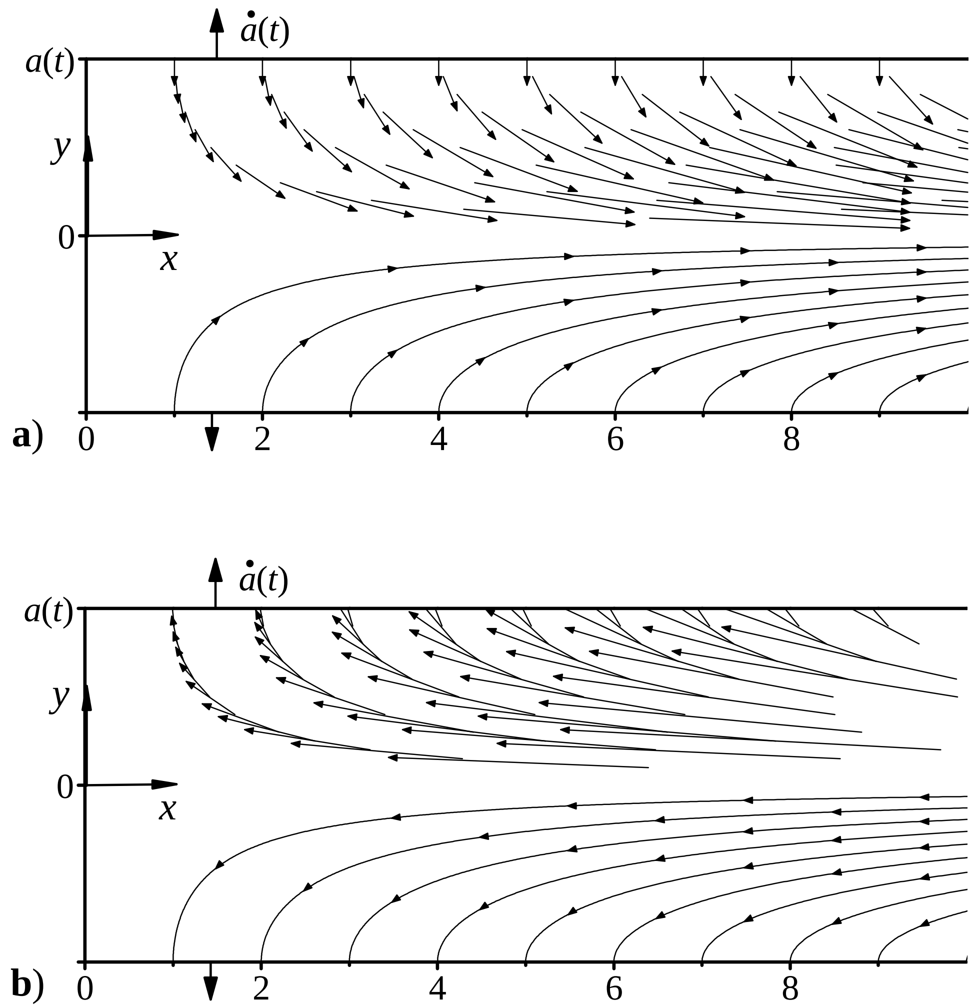

Figure 2. Geometry and dimensional coordinate system associated with a two-dimensional porous channel with a) sidewall injection or b) suction.

In the propulsion community, although the majority of idealized rocket motors comprise circular cross-sections, the Cartesian planar motion associated with a slab rocket motor has become no less popular in recent years. A large number of experimental [32,45-47,53-56] and theoretical investigations [32,55-59] exist in which the 2D assumption is employed. This may be partly attributed to advantages offered by planar configurations such as the ease of computation or flow visualization when the experimental setting requires the use of a windowed environment.

B. Planar Equations

The equations of motion associated with the flow of an incompressible fluid in a channel may be written as

$$\frac{\partial u}{\partial x}+\frac{\partial v}{\partial y}=0,\ \text{(mass conservation)} \tag{2.1}$$

$$\frac{\partial u}{\partial t}+u\frac{\partial u}{\partial x}+v\frac{\partial u}{\partial y}=-\frac{1}{\circ}\frac{\partial p}{\partial x}+\neg\left(\frac{\partial^2 u}{\partial x^2}+\frac{\partial^2 u}{\partial y^2}\right),\ (x\text{-momentum}) \tag{2.2}$$

and

$$\frac{\partial v}{\partial t}+u\frac{\partial v}{\partial x}+v\frac{\partial v}{\partial y}=-\frac{1}{\circ}\frac{\partial p}{\partial y}+\neg\left(\frac{\partial^2 v}{\partial x^2}+\frac{\partial^2 v}{\partial y^2}\right).\ (y\text{-momentum}) \tag{2.3}$$

These are subject to the several key boundary conditions, namely,

$$y=a(t):\quad u=0,\quad v=-V_w, \tag{2.4}$$

where V_w is the absolute speed of injection. This term can be written as $V_w=V_b-\dot{a}$, with V_b being the blowing speed relative to the moving wall. Intuitively, one may see that a contracting wall (i.e., one with a negative wall regression speed $\dot{a}$) will impart an additional component to the incoming fluid. Conversely, an expanding wall will lead to a reduction in the absolute velocity of the injectant. Other boundary conditions include

$$x = 0: \quad \frac{\partial u}{\partial y} = 0, \quad v = 0, \tag{2.5}$$

and

$$y = 0: \quad \frac{\partial u}{\partial y} = 0, \quad v = 0, \tag{2.6}$$

As shown in Fig. 1, Cartesian coordinates (x, y) are used such that the x-axis is taken along the length of the channel and the vertical y-axis in the wall-normal direction. As usual, u and v are taken to represent the two-dimensional velocity components in the x- and y-directions, whereas ρ, p, ν, t, and V_w are set to denote the dimensional density, pressure, kinematic viscosity, time, and the (crossflow) injection speed at the wall. In view of the attendant symmetry about the midsection plane, Eqs. (2.4)-(2.6) are written in the upper half-domain ($y \geq 0$) only.

At this juncture, one may introduce the streamfunction, ψ, using $u = \partial \psi / \partial y$ and $v = -\partial \psi / \partial x$. The conservation of mass relation is immediately fulfilled, thus leaving us with the vorticity transport equation which can be obtained from the curl of the momentum equation. Using ω to define the flow vorticity, one can put

$$\omega = \frac{\partial v}{\partial x} - \frac{\partial u}{\partial y} = -\nabla^2 \psi \tag{2.7}$$

and so

$$\frac{\partial \omega}{\partial t} + u \frac{\partial \omega}{\partial x} + v \frac{\partial \omega}{\partial y} = \nu \left(\frac{\partial^2 \omega}{\partial x^2} + \frac{\partial^2 \omega}{\partial y^2} \right). \tag{2.8}$$

As shown by Dauenhauer and Majdalani [60], one can define two variable transformations, specifically

$$\psi = (\nu x / a) F(\eta, t), \quad \eta = y / a \qquad (2.9)$$

When Eq. (2.9) is substituted into the vorticity transportation equation, careful partial differentiation leads to

$$[F_{\eta\eta\eta} + FF_{\eta\eta} + F_{\eta}(2\alpha - F_{\eta}) + \alpha\eta F_{\eta\eta} - (a^2/\nu)F_{\eta t}]_{\eta} = 0, \qquad (2.10)$$

The boundary conditions given by Eqs. (2.4)-(2.6) become

$$\begin{cases} \eta = 0: \quad F = 0, \quad F_{\eta\eta} = 0 \\ \eta = 1: \quad F = R, \quad F_{\eta} = 0. \end{cases} \qquad (2.11)$$

Equations (2.10)-(2.11) control the motion of an incompressible fluid in a porous channel. It is was first obtained by Dauenhauer and Majdalani [60] and presented in the third edition by White [61] as one of the new exact Navier-Stokes solutions for channel flows. Note that the wall expansion ratio, $\alpha = \dot{a}a/\nu$, appears naturally in Eq. (2.10). Recalling that a and $\dot{a}$ refer to the half-height of the channel and its expansion speed, α represents a Reynolds number based on the regression speed of the sidewalls. With ν being the kinematic viscosity, a connection may be written between the crossflow Reynolds number and α, namely, $R = V_w a/\nu = A\alpha$. The constant of proportionality, A, denotes the so-called injection coefficient. It is important to remark that our sign convention associates a positive R with sidewall injection and a negative R with sidewall suction. The interested reader may refer to Dauenhauer and Majdalani [60], where the intermediate steps leading to Eq. (2.10) are provided with more detail.

A special case arises when the wall expansion ratio, $\sim$, is constant in time. The function F becomes dependent on ¦ and $\sim$ instead of (¦, t). One can put $F_{¦t} = 0$ and write

$$\frac{a\dot{a}}{\neg} = \left(\frac{a\dot{a}}{\neg}\right)_{t=0} = \frac{a_0\dot{a}_0}{\neg} = \sim \tag{2.12}$$

In the above, a_0 and $\dot{a}_0$ are used to designate the initial channel height and expansion rate, respectively. Integration of Eq. (2.12) with respect to t leads to

$$a(t) = a_0\sqrt{1 + 2\frac{\neg\sim}{a_0^2}t} \tag{2.13}$$

Note that the crossflow Reynolds number is based on the absolute speed, namely,

$$R = \frac{V_w a}{\neg} = \frac{(V_b - \dot{a})a}{\neg} = \frac{V_b a}{\neg} - \sim = R_b - \sim \tag{2.14}$$

where R_b is the blowing Reynolds number relative to the regressing grain. Given the time-dependence of $a(t)$, the crossflow Reynolds is generally a function of time. To simplify the upcoming analysis, we limit ourselves to cases for which the absolute crossflow Reynolds number is constant. Based on Eq. (2.14), this implies

$$\frac{V_w a}{\neg} = \left(\frac{V_w a}{\neg}\right)_{t=0} = \frac{V_w(0)a_0}{\neg} = \text{constant} \tag{2.15}$$

whence

$$V_w(t) = \frac{V_w(0)a_0}{a(t)} \tag{2.16}$$

Then using Eq. (2.13), we can put

$$V_w(t) = \frac{V_w(0)}{\sqrt{1+2\nu\alpha t / a_0^2}} \tag{2.17}$$

Finally, recalling that $V_w a / \nu = A\alpha$, we have

$$\frac{V_w a}{\nu} = A \frac{a\dot{a}}{\nu} \quad \text{or} \quad \frac{V_w}{\dot{a}} = A \tag{2.18}$$

By assuming a time-invariant injection coefficient, A, Eqs. (2.17) and (2.18) may be combined to give

$$\frac{V_w(t)}{V_w(0)} = \frac{\dot{a}}{\dot{a}_0} = \frac{1}{\sqrt{1+2\nu\alpha t / a_0^2}}. \tag{2.19}$$

As shown by Dauenhauer and Majdalani [60], a backward substitution of these relations leads to an exact self-similarity equation for Berman's characteristic mean flow function, F. One finds

$$F'''' + \alpha(\eta F''' + 3F'') + FF''' - F'F'' = 0; \quad 0 \le \eta \le 1 \tag{2.20}$$

with

$$F(0) = 0, \quad F''(0) = 0, \quad F(1) = R, \quad F'(1) = 0 \tag{2.21}$$

where $F = F(\eta)$. A further simplification may be realized by defining

$$f = \frac{F}{R} \tag{2.22}$$

This expression transforms Eqs. (2.20)-(2.21) into

$$f'''' + \alpha(\eta f''' + 3f'') + R(ff''' - f'f'') = 0; \quad 0 \le \eta \le 1 \tag{2.23}$$

$$f(0) = f''(0) = f'(1) = 0, \quad f(1) = 1 \tag{2.24}$$

In what follows, this problem will be solved using the Adomian Decomposition Method.

C. Axisymmetric Equations

As shown by Majdalani et al. [62,63], this problem may be repeated in cylindrical geometry (r, z) with the half-height being replaced by the radius of the cylinder. In this case, one can use $\eta = \frac{1}{2} r^2$ to obtain a fourth-order nonlinear ODE:

$$\eta f'''' + \alpha(\eta f''' + 2 f'') + \tfrac{1}{2} R(f f''' - f' f'') + 2 f''' = 0; \quad 0 \le \eta \le \tfrac{1}{2}. \tag{2.25}$$

where, in similar fashion, R represents the sidewall injection Reynolds number, and $\alpha < 1$ denotes the wall expansion ratio. This fourth-order ODE has an assortment of four boundary conditions, specifically

$$f(0) = f'(\tfrac{1}{2}) = 0, \quad f(\tfrac{1}{2}) = 1, \quad \lim_{\eta \to 0}\left(f'' \sqrt{2\eta} \right) = 0 \tag{2.26}$$

Chapter 3

Adomian Decomposition Solution

The cylindrical equation of motion below will be solved using the Adomian Decomposition Method (ADM). The governing equation is as follows:

$$¦ F'''' + \sim \left(¦ F''' + 2F'' \right) + \frac{1}{2} R \left(FF''' - F'F'' \right) + 2F''' = 0 \qquad (3.1)$$

$$0 \le ¦ \le \frac{1}{2} \qquad (3.2)$$

$$\text{Boundary Conditions } : \begin{cases} F(0) = 0 \\ F\left(\frac{1}{2}\right) = 1 \\ F'\left(\frac{1}{2}\right) = 0 \\ \lim\limits_{¦ \to 0} \left(F'' \sqrt{2¦} \right) = 0 \end{cases} \qquad (3.3)$$

A. ADM Setup

First, rewrite the governing equation to isolate the highest derivative of $F(¦)$

$$F'''' = -\sim \left(F''' + \frac{2}{¦} F'' \right) - \frac{1}{2¦} R \left(FF''' - F'F'' \right) - \frac{2}{¦} F''' \qquad (3.4)$$

A differential equation is written as

$$\mathcal{F} u = g(t) \qquad (3.5)$$

where $\mathcal{F}$ is the function dependent on u and $g(t)$ is the forcing function, zero, in this case. Hence, $\mathcal{F}$ can be rewritten as

$$\mathcal{F} u = \mathcal{L} u + \mathcal{N} u \qquad (3.6)$$

where $\mathcal{L}u$ and $\mathcal{N}u$ are the linear and non-linear components of the function, respectively. The linear portion can be further divided into the highest mth derivative, $\mathscr{L}u$ and the remainder of the linear terms, $\mathscr{R}u$, as shown below,

$$\mathcal{L}u = \mathscr{L}u + \mathscr{R}u \tag{3.7}$$

The highest mth order derivative in the governing equation is

$$\mathscr{L}(F) = F'''' \tag{3.8}$$

The remainder is

$$\mathscr{R}(F) = -\text{~}\left(F''' + \frac{2}{\text{¦}}F''\right) - \frac{2}{\text{¦}}F''' \tag{3.9}$$

The non-linear operator is

$$\mathcal{N}(F) = -\frac{R}{2\text{¦}}\left(FF''' - F'F''\right) \tag{3.10}$$

B. Adomian Polynomials

To derive the Adomian Polynomials, $A_0 \ldots A_n$, F, is first expanded as follows:

$$F = \sum_{n=0}^{1} \text{ª}^n F_n = F_0 + \text{ª} F_1 \tag{3.11}$$

$$\mathcal{N}(F) = \mathcal{N}\left(F_0 + \text{ª} F_1 + \ldots\right) \tag{3.12}$$

$$\mathcal{N}(F) = \frac{R}{2\text{¦}}\left(F'F'' - FF'''\right) \tag{3.13}$$

$$\mathcal{N}(F) = \frac{R}{2\text{¦}}\left[\left(F_0' + \text{ª} F_1'\right)\left(F_0'' + \text{ª} F_1''\right) - \left(F_0 + \text{ª} F_1\right)\left(F_0''' + \text{ª} F_1'''\right)\right] . \tag{3.14}$$

Expanding the previous equation and collecting the ª terms,

$$\mathcal{N}\left(F\right)=\frac{R}{2\eta}\left(F_0'F_0''-F_0F_0'''\right)+\frac{R}{2\eta}\lambda\left(F_1''F_0'+F_1'F_0''-F_1'''F_0-F_1F_0'''\right)+O\left(\lambda^2\right) \quad (3.15)$$

The Adomian Polynomials are defined using the general form

$$A_n=\frac{1}{n!}\frac{d^n\mathcal{N}\left(F\left(\lambda\right)\right)}{d\lambda^n}\bigg|_{\lambda=1} \quad (3.16)$$

$$A_0=\frac{1}{n!}\frac{d^0\mathcal{N}\left(F\left(\lambda\right)\right)}{d\lambda^0}\bigg|_{\lambda=1}=\frac{R}{2\eta}\left(F_0'F_0''-F_0F_0'''\right) \quad (3.17)$$

$$A_1=\frac{1}{n!}\frac{d^1\mathcal{N}\left(F\left(\lambda\right)\right)}{d\lambda^1}\bigg|_{\lambda=1}=\frac{R}{2\eta}\left(F_1''F_0'+F_1'F_0''-F_1'''F_0-F_1F_0'''\right) \quad (3.18)$$

C. Adomian Decomposition

Since the highest derivative is of the fourth order, we select an inverse linear operator to be a four-fold integrator:

$$\mathscr{L}F=F''''\Rightarrow\mathscr{L}^{-1}\mathscr{L}F\rightarrow F\left(\eta\right) \quad (3.19)$$

$$\mathscr{L}^{-1}\mathscr{L}F=\mathscr{L}^{-1}\left(F''''\right)=\int_0^{\eta}\left\{\int_{1/2}^{\eta_4}\left[\int_0^{\eta_3}\left(\int_0^{\eta_2}F''''\mathrm{d}\eta_1\right)\mathrm{d}\eta_2\right]\mathrm{d}\eta_3\right\}\mathrm{d}\eta_4 \quad (3.20)$$

$$\begin{aligned}
&=\int_0^{\eta}\left\{\int_{1/2}^{\eta_4}\left[\int_0^{\eta_3}\left(F'''\left(\eta_2\right)-F'''\left(0\right)\right)\mathrm{d}\eta_2\right]\mathrm{d}\eta_3\right\}\mathrm{d}\eta_4\\
&=\int_0^{\eta}\left\{\int_{1/2}^{\eta_4}\left[F''\left(\eta_3\right)-\eta_3F'''\left(0\right)-F''\left(0\right)-\cancel{\left(0\right)F'''\left(0\right)}\right]\mathrm{d}\eta_3\right\}\mathrm{d}\eta_4\\
&=\int_0^{\eta}\left\{F'\left(\eta_4\right)-F'\left(\tfrac{1}{2}\right)-\eta_4F''\left(0\right)+\frac{1}{2}F''\left(0\right)-\frac{\eta_4^2}{2}F'''\left(0\right)+\frac{1}{8}F'''\left(0\right)\right\}\mathrm{d}\eta_4\\
&=F\left(\eta\right)-F\left(0\right)-\eta F'\left(\tfrac{1}{2}\right)-\frac{\eta^2}{2}F''\left(0\right)+\frac{\eta}{2}F''\left(0\right)-\frac{\eta^3}{6}F'''\left(0\right)+\frac{\eta}{8}F'''\left(0\right)
\end{aligned} \quad (3.21)$$

$$\mathcal{L}^{-1}F'''' = F(¦) - ¦^3\underbrace{\left(\frac{1}{6}F'''(0)\right)}_{c_1} - ¦^2\underbrace{\left(\frac{1}{2}F''(0)\right)}_{c_2}$$
$$-¦\underbrace{\left(F'\left(\tfrac{1}{2}\right) - \frac{1}{2}F''(0) - \frac{1}{8}F'''(0)\right)}_{c_3} - \underbrace{\left(F(0)\right)}_{c_4} \tag{3.22}$$

Rewriting the equation and making use of the constants c_1, c_2, c_3, and c_4,

$$F(¦) = \underbrace{\mathcal{L}^{-1}F''''}_{\mathcal{L}(F)=F''''} + ¦^3c_1 + ¦^2c_2 + ¦c_3 + c_4 \tag{3.23}$$

$$\begin{aligned} &\mathcal{L}(F) = \mathcal{R}(F) + \mathcal{N}(F) \\ &\therefore \mathcal{L}^{-1}F'''' = \mathcal{L}^{-1}\mathcal{R}(F) + \mathcal{L}^{-1}\mathcal{N}(F) \end{aligned} \tag{3.24}$$

$$F(¦) = \mathcal{L}^{-1}\mathcal{R}(F) + \mathcal{L}^{-1}\underbrace{\mathcal{N}(F)}_{\mathcal{N}(F)=\sum_{n=0}^{2}A_n} + ¦^3c_1 + ¦^2c_2 + ¦c_3 + c_4 \tag{3.25}$$

For $F = F_0 + F_1 + F_2 + ...$

$$F_0 + F_1 + F_2 = \mathcal{L}^{-1}\left(\mathcal{R}_0 + \mathcal{R}_1 + \mathcal{R}_2\right) + \mathcal{L}^{-1}\left(A_0 + A_1 + A_2\right) + ¦^3c_1 + ¦^2c_2 + ¦c_3 + c_4 \tag{3.26}$$

i. Zeroth Order Solution

The zeroth order solution is defined by the equation

$$F_0 = ¦^3c_1 + ¦^2c_2 + ¦c_3 + c_4 \tag{3.27}$$

Applying the boundary conditions

$$\begin{aligned} &F_0(0) = 0: \\ &0 = (0)c_1 + (0)c_2 + (0)c_3 + c_4 \\ &\Rightarrow c_4 = 0 \end{aligned} \tag{3.28}$$

$$\lim_{¦\to 0}\left(F_0''\sqrt{2¦}\right)=0:$$
$$0=6¦\,c_1\sqrt{2¦}+2\underbrace{c_2}\sqrt{2¦}+0 \tag{3.29}$$

Above, is set as a constant. So far, the zeroth order equation is as follows:

$$F_0=¦^3c_1+¦^2\quad+¦\,c_3 \tag{3.30}$$

Continuing with the remaining boundary conditions,

$$F_0\left(\tfrac{1}{2}\right)=1:$$
$$1=\frac{1}{8}c_1+\frac{1}{4}\quad+\frac{1}{2}c_3 \tag{3.31}$$

$$F_0'\left(\tfrac{1}{2}\right)=0:$$
$$0=3\left(\frac{1}{4}\right)c_1+2\left(\frac{1}{2}\right)\quad+c_3 \tag{3.32}$$

$$\Rightarrow c_3=-\quad-\frac{3}{4}c_1 \tag{3.33}$$

Next, substitute c_3 into the previous boundary condition result,

$$1=\frac{c_1}{8}+\frac{}{4}+\frac{1}{2}\overbrace{\left(-\quad-\frac{3}{4}c_1\right)}^{c_3}$$
$$1=\frac{c_1}{8}+\frac{}{4}-\frac{}{2}-\frac{3c_1}{8} \tag{3.34}$$

$$c_1=-\quad-4 \tag{3.35}$$

Now, substitute the result for constant c_1 back into the c_3 equation:

$$c_3=-\quad-\frac{3}{4}\left(-\quad-4\right)=-\quad+\frac{3}{4}+3 \tag{3.36}$$

$$c_3 = -\frac{\ }{4} + 3 \tag{3.37}$$

$$\Rightarrow F_0 = ¦^3\left(- \quad -4\right) + ¦^2 \quad + ¦\left(-\frac{\ }{4} + 3\right) \tag{3.38}$$

To evaluate , substitute the F_0 equation back into the governing equation:

$$¦F'''' + \sim\left(¦F''' + 2F''\right) + \frac{1}{2}R\left(FF''' - F'F''\right) + 2F''' = 0 \tag{3.39}$$

$$F_0' = 3¦^2\left(- \quad -4\right) + 2¦ \quad + \left(-\frac{\ }{4} + 3\right) \tag{3.40}$$

$$F_0'' = 6¦\left(- \quad -4\right) + 2 \tag{3.41}$$

$$F_0''' = 6\left(- \quad -4\right) = -6 \quad -24 \tag{3.42}$$

$$F_0'''' = 0 \tag{3.43}$$

$$\begin{aligned}
&¦(0) + \sim\left\{¦\left(-6 \quad -24\right) + 2\left[6¦\left(- \quad -4\right) + 2 \quad \right]\right\} \\
&+\frac{1}{2}R\left\{\left[¦^3\left(- \quad -4\right) + ¦^2 \quad + ¦\left(-\frac{\ }{4} + 3\right)\right]\left[-6 \quad -24\right]\right. \\
&\left.-\left[3¦^2\left(- \quad -4\right) + 2¦ \quad + \left(-\frac{\ }{4} + 3\right)\right]\left[6¦\left(- \quad -4\right) + 2 \quad \right]\right\} \\
&+2\left(-6 \quad -24\right) = 0
\end{aligned} \tag{3.44}$$

At the centerline, $¦ = 0$. Therefore, the equation becomes

$$\sim\left[2\left(2 \quad \right)\right] + \frac{1}{2}R\left[0 - \left(-\frac{\ }{4} + 3\right)\left(2 \quad \right)\right] + 2\left(-6 \quad -24\right) = 0 \tag{3.45}$$

$$\sim 4 \quad + R\left(\frac{\ ^2}{4} - 3 \quad \right) + \left(-12 \quad -48\right) = 0 \tag{3.46}$$

$$\sim 4 \quad + \frac{R}{4} \quad ^{2} - 3R \quad - 12 \quad - 48 = 0 \tag{3.47}$$

$$-48 + \left(4\sim - 3R - 12\right) \quad + \frac{R}{4} \quad ^{2} = 0 \tag{3.48}$$

Using the quadratic formula to solve for   in the above equation, we get

$$_{1} = \frac{48 + 12R - 16\sim - \sqrt{768R + \left(-48 - 12R + 16\sim\right)^{2}}}{2R} \tag{3.49}$$

$$_{2} = \frac{48 + 12R - 16\sim + \sqrt{768R + \left(-48 - 12R + 16\sim\right)^{2}}}{2R} \tag{3.50}$$

After plotting, the only physical value for   is $_{1}$. Now substituting   into the F_0 equation, the resulting zeroth order solution equation is shown below:

$$\boxed{\begin{aligned} F_0 = ¦^{3} & \left[-\left(\frac{48 + 12R - 16\sim - \sqrt{768R + \left(-48 - 12R + 16\sim\right)^{2}}}{2R} \right) - 4 \right] \\ +¦^{2} & \left(\frac{48 + 12R - 16\sim - \sqrt{768R + \left(-48 - 12R + 16\sim\right)^{2}}}{2R} \right) \\ +¦ & \left[-\frac{1}{4}\left(\frac{48 + 12R - 16\sim - \sqrt{768R + \left(-48 - 12R + 16\sim\right)^{2}}}{2R} \right) + 3 \right] \end{aligned}} \tag{3.51}$$

ii. First Order Solution

The first order solution is defined by the following equation:

$$F_1 = \mathscr{L}^{-1}\left(\mathscr{R}_0\right) + \mathscr{L}^{-1}\left(A_0\right) \ . \tag{3.52}$$

The zeroth order equation is simplified by substituting in for the constants:

$$
\begin{aligned}
F_0 &= x_1 ¦ + x_2 ¦^2 + x_3 ¦^3 \\
x_1 &= -\frac{6}{R} + \frac{3}{2} + \frac{2\sim}{R} - \frac{\sqrt{768R + \left(-48 - 12R + 16\sim\right)^2}}{2R} \\
x_2 &= \frac{24}{R} + 6 - \frac{8\sim}{R} - \frac{\sqrt{768R + \left(-48 - 12R + 16\sim\right)^2}}{2R} \\
x_3 &= -\frac{24}{R} - 10 + \frac{8\sim}{R} - \frac{\sqrt{768R + \left(-48 - 12R + 16\sim\right)^2}}{2R}
\end{aligned}
\tag{3.53}
$$

Recalling the equation for the zeroth order Adomian polynomial, the derivatives of the F_0 equation are required and thus calculated,

$$A_0 = \frac{R}{2¦}\left(F_0' F_0'' - F_0 F_0'''\right) \tag{3.54}$$

$$F_0 = x_1 ¦ + x_2 ¦^2 + x_3 ¦^3 \tag{3.55}$$

$$F_0' = x_1 + 2x_2 ¦ + 3x_3 ¦^2 \tag{3.56}$$

$$F_0'' = 0 + 2x_2 + 6x_3 ¦ \tag{3.57}$$

$$F_0''' = 0 + 0 + 6x_3 \tag{3.58}$$

$$
\begin{aligned}
\therefore A_0 = \frac{R}{2¦}\Big[&\left(x_1 + 2x_2 ¦ + 3x_3 ¦^2\right)\left(2x_2 + 6x_3 ¦\right) \\
&-\left(x_1 ¦ + x_2 ¦^2 + x_3 ¦^3\right)\left(6x_3\right)\Big]
\end{aligned}
\tag{3.59}
$$

$$= \frac{R}{2¦}\left[2x_1 x_2 + 4x_2^2 ¦ + 12x_2 x_3 ¦^2 + 12x_3^2 ¦^3\right] \tag{3.60}$$

$$A_0 = R\left[\frac{x_1 x_2}{¦} + 2x_2^2 + 6x_2 x_3 ¦ + 6x_3^2 ¦^2\right] \tag{3.61}$$

Next, recall the equation for the remainder of the linear portion of F :

$$\mathcal{R}_0(F) = -\sim\left(F_0''' + \frac{2}{¦}F_0''\right) - \frac{2}{¦}F''' \tag{3.62}$$

$$= -\sim\left[6x_3 + \frac{2}{¦}\left(2x_2 + 6x_3¦\right)\right] - \frac{2}{¦}\left(6x_3\right) \tag{3.63}$$

$$= -\sim\left[6x_3 + \frac{4}{¦}x_2 + 12x_3\right] - \frac{12}{¦}x_3 \tag{3.64}$$

$$\mathcal{R}_0 = -18x_3\sim + \frac{-4x_2\sim - 12x_3}{¦} \tag{3.65}$$

Going back to the F_1 equation,

$$F_1 = \mathcal{L}^{-1}\left(\mathcal{R}_0\right) + \mathcal{L}^{-1}\left(A_0\right) = \mathcal{L}^{-1}\left(\mathcal{R}_0 + A_0\right) \tag{3.66}$$

$$\begin{aligned} &= \mathcal{L}^{-1}\left(-18x_3\sim + \frac{-4x_2\sim - 12x_3}{¦}\right. \\ &\left. + \frac{x_1x_2}{¦}R + 2x_2^2R + 6x_2x_3¦R + 6x_3^2¦^2R\right) \end{aligned} \tag{3.67}$$

$$\begin{aligned} &= \mathcal{L}^{-1}\left(\frac{1}{¦}\left(-4x_2\sim - 12x_3 + x_1x_2R\right)\right. \\ &\left. + \left(2x_2^2R - 18x_3\sim\right) + 6x_2x_3¦R + 6x_3^2¦^2R\right) \end{aligned} \tag{3.68}$$

Once again, using a four-fold integration as the inverse linear operator, F_1, is calculated:

$$\begin{aligned} F_1 &= \frac{1}{12}\left(Rx_2^2 - 9x_3\sim\right)¦^4 + \frac{1}{20}Rx_2x_3¦^5 + \frac{1}{60}Rx_3^2¦^6 \\ &+ ¦^3\left[-\frac{11}{36}Rx_1x_2 + \frac{11}{3}x_3 + \frac{11}{9}x_2\sim + \frac{1}{6}\left(Rx_1x_2 - 12x_3 - 4x_2\sim\right)\ln\left(¦\right)\right] \\ &+ d_1¦^3 + d_2¦^2 + d_3¦ + d_4 \end{aligned} \tag{3.69}$$

Next, find the derivatives of F_1, and apply the boundary conditions:

$$F_1 = \frac{1}{12}\left(Rx_2^2 - 9x_3\sim\right)\brvbar^4 + \frac{1}{20}Rx_2x_3\brvbar^5 + \frac{1}{60}Rx_3^2\brvbar^6$$
$$+\frac{1}{6}\left(Rx_1x_2 - 12x_3 - 4x_2\sim\right)\brvbar^3\ln\left(\brvbar\right) + \left(-\frac{11}{36}Rx_1x_2 + \frac{11}{3}x_3 + \frac{11}{9}x_2\sim\right)\brvbar^3 \quad (3.70)$$
$$+d_1\brvbar^3 + d_2\brvbar^2 + d_3\brvbar + d_4$$

$$F_1' = \frac{1}{6}\left(Rx_1x_2 - 12x_3 - 4x_2\sim\right)\brvbar^2 + \frac{1}{3}\left(Rx_2^2 - 9x_3\sim\right)\brvbar^3 + \frac{1}{4}Rx_2x_3\brvbar^4$$
$$+\frac{1}{10}Rx_3^2\brvbar^5 + \frac{1}{2}\left(Rx_1x_2 - 12x_3 - 4x_2\sim\right)\brvbar^2\ln\left(\brvbar\right) \quad (3.71)$$
$$+3\left(-\frac{11}{36}Rx_1x_2 + \frac{11}{3}x_3 + \frac{11}{9}x_2\sim\right)\brvbar^2 + 3d_1\brvbar^2 + 2d_2\brvbar + d_3$$

$$F_1'' = \frac{5}{6}\left(Rx_1x_2 - 12x_3 - 4x_2\sim\right)\brvbar + \left(Rx_2^2 - 9x_3\sim\right)\brvbar^2 + Rx_2x_3\brvbar^3$$
$$+\frac{1}{2}Rx_3^2\brvbar^4 + \left(Rx_1x_2 - 12x_3 - 4x_2\sim\right)\brvbar\ln\left(\brvbar\right) \quad (3.72)$$
$$+6\left(-\frac{11}{36}Rx_1x_2 + \frac{11}{3}x_3 + \frac{11}{9}x_2\sim\right)\brvbar + 6d_1\brvbar + 2d_2$$

$$\lim_{\brvbar\to 0} F_1 = 0:$$
$$\Rightarrow d_4 = 0 \quad (3.73)$$

$$\lim_{\brvbar\to 0}\left(F_1''\sqrt{2\brvbar}\right) = 0:$$
$$\Rightarrow d_2 = 0 \quad (3.74)$$

$$F_1\left(\tfrac{1}{2}\right) = 1:$$
$$1 = \frac{1}{12}\left(Rx_2^2 - 9x_3\sim\right)\left(\frac{1}{16}\right) + \frac{1}{20}Rx_2x_3\left(\frac{1}{32}\right) + \frac{1}{60}Rx_3^2\left(\frac{1}{64}\right)$$
$$+\frac{1}{6}\left(Rx_1x_2 - 12x_3 - 4x_2\sim\right)\left(\frac{1}{8}\right)\left(-\ln\left(2\right)\right) \quad (3.75)$$
$$+\left(-\frac{11}{36}Rx_1x_2 + \frac{11}{3}x_3 + \frac{11}{9}x_2\sim\right)\left(\frac{1}{8}\right) + d_1\left(\frac{1}{8}\right) + d_3\left(\frac{1}{2}\right)$$

$$
\begin{aligned}
1 = {} & \frac{1}{192}Rx_2^2 - \frac{9}{192}x_3\sim + \frac{1}{640}Rx_2x_3 + \frac{1}{3840}Rx_3^2 \\
& - \frac{1}{48}\left(Rx_1x_2 - 12x_3 - 4x_2\sim\right)\left(-\ln(2)\right) \\
& - \frac{11}{288}Rx_1x_2 + \frac{11}{24}x_3 + \frac{11}{72}x_2\sim + \frac{1}{8}d_1 + \frac{1}{2}d_3
\end{aligned}
\tag{3.76}
$$

$F_1'\left(\tfrac{1}{2}\right) = 0$:

$$
\begin{aligned}
0 = {} & \frac{1}{3}\left(Rx_2^2 - 9x_3\sim\right)\left(\frac{1}{8}\right) + \frac{1}{4}Rx_2x_3\left(\frac{1}{16}\right) + \frac{1}{10}Rx_3^2\left(\frac{1}{32}\right) \\
& + \frac{1}{6}\left(Rx_1x_2 - 12x_3 - 4x_2\sim\right)\left(\frac{1}{4}\right)\left(-3\ln(2) + 1\right) \\
& + 3\left(-\frac{11}{36}Rx_1x_2 + \frac{11}{3}x_3 + \frac{11}{9}x_2\sim\right)\left(\frac{1}{4}\right) + \left(\frac{3}{4}\right)d_1 + d_3
\end{aligned}
\tag{3.77}
$$

Solving the system of equations above, the solutions for d_1 and d_3 result:

$$
\begin{aligned}
d_1 = {} & \frac{1}{2880}\Big(-11520 + 1520Rx_1x_2 - 180Rx_2^2 + 2880x_3 \\
& - 72Rx_2x_3 - 15Rx_3^2 - 6080x_2\sim + 1620x_3\sim \\
& + 480Rx_1x_2\ln(2) - 5760x_3\ln(2) - 1920x_2\sim\ln(2)\Big)
\end{aligned}
\tag{3.78}
$$

$$
\begin{aligned}
d_3 = {} & \frac{1}{3840}\Big(11520 + 80Rx_1x_2 + 20Rx_2^2 - 960x_3 \\
& + 12Rx_2x_3 + 3Rx_3^2 - 320x_2\sim - 180x_3\sim\Big)
\end{aligned}
\tag{3.79}
$$

Finally, the First Order Solution, F_1, is obtained:

$$
\boxed{
\begin{aligned}
F_1 = {} & \frac{1}{12}\left(Rx_2^2 - 9x_3\sim\right)¦^4 + \frac{1}{20}Rx_2x_3¦^5 + \frac{1}{60}Rx_3^2¦^6 \\
& + \frac{1}{6}\left(Rx_1x_2 - 12x_3 - 4x_2\sim\right)¦^3\ln(¦) + d_1¦^3 + d_3¦
\end{aligned}
}
\tag{3.80}
$$

To set up the second order solution, the constants are rewritten as shown next:

$$F_1 = \underbrace{\left(\frac{1}{60}Rx_3^2\right)}_{y_1}¦^6 + \underbrace{\left(\frac{1}{20}Rx_2x_3\right)}_{y_2}¦^5 + \underbrace{\left[\frac{1}{12}\left(Rx_2^2 - 9x_3\sim\right)\right]}_{y_3}¦^4$$
$$+\underbrace{\left[\frac{1}{6}\left(Rx_1x_2 - 12x_3 - 4x_2\sim\right)\right]}_{y_4}¦^3 \ln(¦) + d_1¦^3 + d_3¦ \tag{3.81}$$

$$F_1 = y_1¦^6 + y_2¦^5 + y_3¦^4 + y_4¦^3 \ln(¦) + d_1¦^3 + d_3¦ \tag{3.82}$$

iii. Second Order Solution

The second order solution is defined by the following equation:

$$F_2 = \mathscr{L}^{-1}\left(\mathscr{R}_1\right) + \mathscr{L}^{-1}\left(A_1\right). \tag{3.83}$$

The zeroth and first order equations are rewritten below, along with the definition of the Adomian polynomial, A_1:

$$F_0 = x_1¦ + x_2¦^2 + x_3¦^3 \tag{3.84}$$

$$F_1 = y_1¦^6 + y_2¦^5 + y_3¦^4 + y_4¦^3 \ln(¦) + d_1¦^3 + d_3¦ \tag{3.85}$$

$$A_1 = \frac{R}{2¦}\left(F_1''F_0' + F_1'F_0'' - F_1'''F_0 - F_1F_0'''\right) \tag{3.86}$$

Next, the first, second, and third derivatives are found for the zeroth and first order equations:

$$F_0' = x_1 + 2x_2¦ + 3x_3¦^2 \tag{3.87}$$

$$F_0'' = 2x_2 + 6x_3¦ \tag{3.88}$$

$$F_0''' = 6x_3 \tag{3.89}$$

$$F_1' = 6y_1¦^5 + 5y_2¦^4 + 4y_3¦^3 + y_4¦^2 + 3y_4¦^2 \ln(¦) + 3d_1¦^2 + d_3 \tag{3.90}$$

$$F_1'' = 30y_1¦^4 + 20y_2¦^3 + 12y_3¦^2 + 5y_4¦ + 6y_4¦\ln(¦) + 6d_1¦ \quad (3.91)$$

$$F_1''' = 120y_1¦^3 + 60y_2¦^2 + 24y_3¦ + 6y_4\ln(¦) + 11y_4 + 6d_1. \quad (3.92)$$

Substituting the appropriate equations into the A_1 equation,

$$\begin{aligned} A_1 &= \frac{1}{2}R(-48x_2y_1 + 24x_3y_2)¦^4 \\ &+ \frac{1}{2}R(-90x_1y_1 - 10x_2y_2 + 30x_3y_3)¦^3 \\ &+ \frac{1}{2}R(24d_1x_3 - 40x_1y_2 + 8x_2y_3 + 10x_3y_4 + 24x_3y_4\ln(¦))¦^2 \\ &+ \frac{1}{2}R(12d_1x_2 - 12x_1y_3 + x_2y_4 + 12x_2y_4\ln(¦))¦ \\ &- 3Rx_1y_4 + \frac{d_3Rx_2}{¦} \end{aligned} \quad (3.93)$$

Once again, recall the equation for the remainder of the linear portion of F, and substitute in the relevant equations for the derivatives of the first order solution,

$$\mathcal{R}_1(F) = -\sim\left(F_1'''' + \frac{2}{¦}F_1''\right) - \frac{2}{¦}F_1''' \quad (3.94)$$

$$\begin{aligned} \mathcal{R}_1 &= -180y_1\sim¦^3 + (-240y_1 - 100y_2\sim)¦^2 \\ &+ (-120y_2 - 48y_3\sim)¦ - 18y_4\sim\ln(¦) \\ &+ \frac{1}{¦}(-12d_1 - 22y_4 - 12y_4\ln(¦)) - 48y_3 - 18d_1\sim - 21y_4\sim \end{aligned} \quad (3.95)$$

Before applying the inverse linear operator, add $\mathcal{R}_1$ and A_1:

$$\mathscr{R}_1 + A_1 = \left(-24Rx_2y_1 + 12Rx_3y_2\right)¦^4$$
$$+\left(-45Rx_1y_1 - 5Rx_2y_2 + 15Rx_3y_3 - 180y_1\sim\right)¦^3$$
$$+\left(12d_1Rx_3 - 240y_1 - 20Rx_1y_2\right.$$
$$\left. +4Rx_2y_3 + 5Rx_3y_4 - 100y_2\sim + 12Rx_3y_4\ln\left(¦\right)\right)¦^2 \tag{3.96}$$
$$+\left(6d_1Rx_2 - 120y_2 - 6Rx_1y_3 + \frac{1}{2}\left(Rx_2y_4\right) - 48y_3\sim + 6Rx_2y_4\ln\left(¦\right)\right)¦$$
$$+\left(-12d_1 + d_3Rx_2 - 22y_4 - 12y_4\ln\left(¦\right)\right)\frac{1}{¦} - 18y_4\sim\ln\left(¦\right)$$
$$-48y_3 - 3Rx_1y_4 - 18d_1\sim - 21y_4\sim$$

To simplify the previous equation, replace the constants as follows:

$$\begin{cases} g_1 = -12d_1 + d_3Rx_2 - 22y_4 \\ g_2 = -48y_3 - 3Rx_1y_4 - 18d_1\sim - 21y_4\sim \\ g_3 = 6d_1Rx_2 - 120y_2 - 6Rx_1y_3 + \frac{1}{2}\left(Rx_2y_4\right) - 48y_3\sim \\ g_4 = 12d_1Rx_3 - 240y_1 - 20Rx_1y_2 + 4Rx_2y_3 + 5Rx_3y_4 - 100y_2\sim \\ g_5 = -45Rx_1y_1 - 5Rx_2y_2 + 15Rx_3y_3 - 180y_1\sim \\ g_6 = -24Rx_2y_1 + 12Rx_3y_2 \end{cases} \tag{3.97}$$

$$\Rightarrow \mathscr{R}_1 + A_1 = g_6¦^4 + g_5¦^3 + ¦^2\left(g_4 + 12Rx_3y_4\ln\left(¦\right)\right)$$
$$+¦\left(g_3 + 6Rx_2y_4\ln\left(¦\right)\right) + g_2 + \frac{1}{¦}\left(g_1 - 12y_4\ln\left(¦\right)\right) \;. \tag{3.98}$$
$$-18y_4\sim\ln\left(¦\right)$$

Now apply the inverse linear operator to the previous sum in order to find F_2:

$$
\begin{aligned}
F_2 &= \mathscr{L}^{-1}\left(\mathscr{R}_1 + A_1\right) \\
&= \frac{g_6}{1680}¦^{8} + \frac{g_5}{840}¦^{7} + \left(\frac{g_4}{360} - \frac{19Rx_3y_4}{600} + \frac{1}{30}Rx_3y_4\ln(¦)\right)¦^{6} \\
&+\left(\frac{g_3}{120} - \frac{77Rx_2y_4}{1200} + \frac{1}{20}Rx_2y_4\ln(¦)\right)¦^{5} \\
&+\left(\frac{g_2}{24} + \frac{25y_4\sim}{16} - \frac{3}{4}y_4\sim\ln(¦)\right)¦^{4} \\
&+\left(-\frac{11g_1}{36} - \frac{85y_4}{18} + \frac{1}{6}g_1\ln(¦) + \frac{11}{3}y_4\ln(¦) - y_4\ln(¦)^2\right)¦^{3} \\
&+e_1 + e_2¦ + e_3¦^{2} + e_4¦^{3}
\end{aligned}
\tag{3.99}
$$

To solve for the constants of integration, $e_1 \rightarrow e_4$, the boundary conditions are once again employed. Before that takes place, the first and second derivatives of the current form of F_2 are calculated,

$$
\begin{aligned}
F_2' &= \frac{g_6}{210}¦^{7} + \frac{g_5}{120}¦^{6} \\
&+\left(\frac{Rx_3y_4}{30} + 6\left(\frac{g_4}{360} - \frac{19Rx_3y_4}{600} + \frac{1}{30}Rx_3y_4\ln(¦)\right)\right)¦^{5} \\
&+\left(\frac{Rx_2y_4}{20} + 5\left(\frac{g_3}{120} - \frac{77Rx_2y_4}{1200} + \frac{1}{20}Rx_2y_4\ln(¦)\right)\right)¦^{4} \\
&+\left(-\frac{3y_4\sim}{4} + 4\left(\frac{g_2}{24} + \frac{25y_4\sim}{16} - \frac{3}{4}y_4\sim\ln(¦)\right)\right)¦^{3} \\
&+\left(3e_4 + \frac{g_1}{6} + \frac{11y_4}{3} - 2y_4\ln(¦)\right. \\
&\left.+3\left(-\frac{11g_1}{36} - \frac{85y_4}{18} + \frac{1}{6}g_1\ln(¦) + \frac{11}{3}y_4\ln(¦) - y_4\ln(¦)^2\right)\right)¦^{2} + e_2
\end{aligned}
\tag{3.100}
$$

$$
\begin{aligned}
F_2'' &= \frac{g_6}{30}¦^{6} + \frac{g_5}{20}¦^{5} \\
&+\left(\frac{11Rx_3y_4}{30} + 30\left(\frac{g_4}{360} - \frac{19Rx_3y_4}{600} + \frac{1}{30}Rx_3y_4\ln(¦)\right)\right)¦^{4} \\
&+\left(\frac{9Rx_2y_4}{20} + 20\left(\frac{g_3}{120} - \frac{77Rx_2y_4}{1200} + \frac{1}{20}Rx_2y_4\ln(¦)\right)\right)¦^{3} \\
&+\left(-\frac{21y_4\sim}{4} + 12\left(\frac{g_2}{24} + \frac{25y_4\sim}{16} - \frac{3}{4}y_4\sim\ln(¦)\right)\right)¦^{2} \\
&+\left(6e_4 + \frac{5g_1}{6} + \frac{49y_4}{3} - 10y_4\ln(¦)\right. \\
&\left.+6\left(-\frac{11g_1}{36} - \frac{85y_4}{18} + \frac{1}{6}g_1\ln(¦) + \frac{11}{3}y_4\ln(¦) - y_4\ln(¦)^2\right)\right)¦
\end{aligned}
\tag{3.101}
$$

Below, the boundary conditions are once again applied:

$$
\begin{aligned}
&\lim_{¦\to 0} F_2 = 0: \\
&\Rightarrow e_1 = 0
\end{aligned}
\tag{3.102}
$$

$$
\begin{aligned}
&\lim_{¦\to 0}\left(F_2''\sqrt{2¦}\right) = 0: \\
&\Rightarrow e_3 = 0
\end{aligned}
\tag{3.103}
$$

The remaining boundary conditions, $F_2\left(\frac{1}{2}\right)=1$ and $F_2'\left(\frac{1}{2}\right)=0$, produce equations that must be solved simultaneously. Solving the system of equations results in the solutions to the constants of integration e_2 and e_4:

$$
\begin{aligned}
e_2 = \frac{1}{2150400}&\left(6451200 + 44800g_1 + 5600g_2 + 1120g_3\right. \\
&+280g_4 + 80g_5 + 25g_6 + 985600y_4 - 5264Rx_2y_4 \\
&-2072Rx_3y_4 + 109200y_4\sim + 537600y_4\ln(2) \\
&\left.-6720Rx_2y_4\ln(2) - 3360Rx_3y_4\ln(2) + 100800y_4\sim\ln(2)\right)
\end{aligned}
\tag{3.104}
$$

$$
\begin{aligned}
e_4 = \frac{1}{1612800}\Big(&-6451200 + 358400 g_1 - 50400 g_2 \\
&-6720 g_3 - 1400 g_4 - 360 g_5 - 105 g_6 + 4659200 y_4 \\
&+41664 R x_2 y_4 + 12600 R x_3 y_4 - 1587600 y_4 \sim \\
&+268800 g_1 \ln(2) + 4300800 y_4 \ln(2) \\
&+40320 R x_2 y_4 \ln(2) + 16800 R x_3 y_4 \ln(2) \\
&-907200 y_4 \sim \ln(2) + 1612800 y_4 \ln(2)^2 \Big)
\end{aligned}
\tag{3.105}
$$

This completes the Second Order solution:

$$
\boxed{
\begin{aligned}
F_2 = &\frac{g_6}{1680} ¦^{8} + \frac{g_5}{840} ¦^{7} \\
&+\left(\frac{g_4}{360} - \frac{19 R x_3 y_4}{600} + \frac{1}{30} R x_3 y_4 \ln(¦)\right) ¦^{6} \\
&+\left(\frac{g_3}{120} - \frac{77 R x_2 y_4}{1200} + \frac{1}{20} R x_2 y_4 \ln(¦)\right) ¦^{5} \\
&+\left(\frac{g_2}{24} + \frac{25 y_4 \sim}{16} - \frac{3}{4} y_4 \sim \ln(¦)\right) ¦^{4} \\
&+\left(-\frac{11 g_1}{36} - \frac{85 y_4}{18} + \frac{1}{6} g_1 \ln(¦) + \frac{11}{3} y_4 \ln(¦) - y_4 \ln(¦)^2\right) ¦^{3} \\
&+e_4 ¦^{3} + e_2 ¦
\end{aligned}
}
\tag{3.106}
$$

iv. Adomian Decomposition Solution

Taking the zeroth, first, and second order solutions to F, we can combine them to form the complete solution,

$$F = F_0 + F_1 + F_2 \tag{3.107}$$

where

$$F_0 = ¦^3 \left[-\left(\frac{48+12R-16\sim - \sqrt{768R+\left(-48-12R+16\sim\right)^2}}{2R} \right) - 4 \right]$$
$$+¦^2 \left(\frac{48+12R-16\sim - \sqrt{768R+\left(-48-12R+16\sim\right)^2}}{2R} \right) \tag{3.108}$$
$$+¦ \left[-\frac{1}{4}\left(\frac{48+12R-16\sim - \sqrt{768R+\left(-48-12R+16\sim\right)^2}}{2R} \right) + 3 \right]$$

$$F_1 = \frac{1}{12}\left(Rx_2^2 - 9x_3\sim\right)¦^4 + \frac{1}{20}Rx_2x_3¦^5 + \frac{1}{60}Rx_3^2¦^6$$
$$+\frac{1}{6}\left(Rx_1x_2 - 12x_3 - 4x_2\sim\right)¦^3 \ln\left(¦\right) + d_1¦^3 + d_3¦ \tag{3.109}$$

$$F_2 = \frac{g_6}{1680}¦^8 + \frac{g_5}{840}¦^7$$
$$+\left(\frac{g_4}{360} - \frac{19Rx_3y_4}{600} + \frac{1}{30}Rx_3y_4\ln\left(¦\right)\right)¦^6$$
$$+\left(\frac{g_3}{120} - \frac{77Rx_2y_4}{1200} + \frac{1}{20}Rx_2y_4\ln\left(¦\right)\right)¦^5 \tag{3.110}$$
$$+\left(\frac{g_2}{24} + \frac{25y_4\sim}{16} - \frac{3}{4}y_4\sim\ln\left(¦\right)\right)¦^4$$
$$+\left(-\frac{11g_1}{36} - \frac{85y_4}{18} + \frac{1}{6}g_1\ln\left(¦\right) + \frac{11}{3}y_4\ln\left(¦\right) - y_4\ln\left(¦\right)^2\right)¦^3$$
$$+e_4¦^3 + e_2¦$$

Chapter 4

Asymptotic Solution

The flow motion in a uniformly porous cylinder with expanding or contracting sidewalls can be used to simulate the motion in a solid rocket motor. Here, the cylindrical case for a small injection or suction is addressed. It can be described by a fourth-order, nonlinear ordinary differential equation (ODE) developed by Majdalani et al. [1,2]:

$$\eta F'''' + \alpha\left(\eta F''' + 2F''\right) + \frac{1}{2}R\left(FF''' - F'F''\right) + 2F''' = 0 \qquad (4.1)$$

$$0 \le \eta \le \frac{1}{2}$$

where R represents the sidewall injection Reynolds number, and $\alpha < 1$ denotes the wall expansion ratio (a small Reynolds number based on the expansion speed of the sidewall). The fourth-order ODE has an assortment of four boundary conditions, specifically

$$\text{Boundary Conditions: } \begin{cases} F(0) = 0 \\ F\left(\frac{1}{2}\right) = 1 \\ F'\left(\frac{1}{2}\right) = 0 \\ \lim\limits_{\eta \to 0}\left(F''\sqrt{2\eta}\right) = 0 \end{cases} \qquad (4.2)$$

A. Double Perturbation Method

For small injection or suction, we can let $\varepsilon \equiv R$ and assume that α is a secondary perturbation parameter. This will enable us to find

$F = F_0 + £ F_1 + O(£^2)$ by interlacing a double perturbation expansion of the form $F_0 = F_{00} + \sim F_{01} + O(\sim^2)$ and $F_1 = F_{10} + \sim F_{11} + O(\sim^2)$. Begin by rewriting the governing equation below:

$$¦ F^{(4)} + \sim\left(¦ F^{(3)} + 2F''\right) + \frac{1}{2}£\left(FF^{(3)} - F'F''\right) + 2F^{(3)} = 0 \qquad (4.3)$$

Substitute the following for F :

$$F = F_0 + £ F_1 + ... \qquad (4.4)$$

$$¦ \left(F_0 + £ F_1\right)^{(4)} + \sim\left(¦ \left(F_0 + £ F_1\right)^{(3)} + 2\left(F_0 + £ F_1\right)''\right) +$$

$$\frac{1}{2}£\left(\left(F_0 + £ F_1\right)\left(F_0 + £ F_1\right)^{(3)} - \left(F_0 + £ F_1\right)' \left(F_0 + £ F_1\right)''\right) + 2\left(F_0 + £ F_1\right)^{(3)} = 0 . \qquad (4.5)$$

Expand the equation, and collect the $£$ terms:

$$¦ F_0^{(4)} + £ ¦ F_1^{(4)} + \sim ¦ F_0^{(3)} + £\sim ¦ F_1^{(3)} + \sim 2F_0'' + £\sim 2F_1'' + \frac{1}{2}£ F_0 F_0^{(3)} + \frac{1}{2}£^2 F_1 F_0^{(3)} + \frac{1}{2}£^2 F_0 F_1^{(3)} +$$

$$\frac{1}{2}£^3 F_1 F_1^{(3)} - \frac{1}{2}£ F_0' F_0'' - \frac{1}{2}£^2 F_1' F_0'' - \frac{1}{2}£^2 F_0' F_1'' - \frac{1}{2}£^3 F_1' F_1'' + 2F_0^{(3)} + 2£ F_1^{(3)} = 0 \qquad (4.6)$$

$$\underbrace{¦ F_0^{(4)} + \sim ¦ F_0^{(3)} + \sim 2F_0'' + 2F_0^{(3)}}_{\text{Leading Order}} +$$

$$\underbrace{£\left(¦ F_1^{(4)} + \sim ¦ F_1^{(3)} + \sim 2F_1'' + \frac{1}{2}F_0 F_0^{(3)} - \frac{1}{2}F_0' F_0'' + 2F_1^{(3)}\right)}_{\text{First Order}} + O\left(£^2\right) = 0 \qquad (4.7)$$

B. Leading Order Solution

To solve for the leading order equation, substitute for F_0 using the following equation with the secondary perturbation parameter of ~ . Expand the equation and collect the ~ terms,

$$\underbrace{¦ F_0^{(4)} + ~ ¦ F_0^{(3)} + ~ 2F_0'' + 2F_0^{(3)}}_{\text{Leading Order}} = 0 \tag{4.8}$$

$$F_0 = F_{00} + ~ F_{01} + ... \tag{4.9}$$

$$¦ F_{00}^{(4)} + ¦ ~ F_{01}^{(4)} + ~ ¦ F_{00}^{(3)} + ~^2 ¦ F_{01}^{(3)} + ~ 2F_{00}'' + ~^2 2F_{01}'' + 2F_{00}^{(3)} + ~ 2F_{01}^{(3)} = 0 \tag{4.10}$$

$$\underbrace{¦ F_{00}^{(4)} + 2F_{00}^{(3)}}_{\substack{\text{Leading Order} \\ \text{Zero Term}}} + ~ \underbrace{\left(¦ F_{01}^{(4)} + ¦ F_{00}^{(3)} + 2F_{00}'' + 2F_{01}^{(3)} \right)}_{\substack{\text{Leading Order} \\ \text{First Term}}} + O\left(~^2\right) = 0 \tag{4.11}$$

i. Leading Order Zero Equation

Solve the linear ordinary differential equation (leading order zero equation), and apply the boundary conditions:

$$\underbrace{¦ F_{00}^{(4)} + 2F_{00}^{(3)} = 0}_{\substack{\text{Leading Order} \\ \text{Zero Equation}}} \tag{4.12}$$

$$F_{00} = c_1 + ¦ c_2 + ¦^2 c_3 + c_4 \left(¦ - ¦ \ln\left(¦ \right) \right) \tag{4.13}$$

$$F_{00}\left(0\right) = 0 \rightarrow c_1 = 0 \rightarrow F_{00} = ¦ c_2 + ¦^2 c_3 + c_4 \left(¦ - ¦ \ln\left(¦ \right) \right) \tag{4.14}$$

$$\lim_{¦ \rightarrow 0}\left(F_{00}'' \sqrt{2¦} \right) = \sqrt{2}\left(-\frac{c_4}{\sqrt{¦}} + 2\, c_3 \sqrt{¦} \right) = 0 \rightarrow c_4 = 0 \rightarrow F_{00} = ¦ c_2 + ¦^2 c_3$$

$$F_{00}'\left(\tfrac{1}{2}\right) = c_2 + c_3 = 0 \rightarrow c_2 = -c_3$$

$$F_{00}\left(\tfrac{1}{2}\right)=1\rightarrow\frac{c_2}{2}+\frac{c_3}{4}=1\rightarrow c_3=-4\ \&\ c_2=4$$

$$\boxed{F_{00}=4\eta-4\eta^2} \qquad (4.15)$$

ii. Leading Order First Equation

Substitute equation (4.15) into the leading order first equation,

$$\eta F_{01}^{(4)}+2F_{01}^{(3)}=-\eta F_{00}^{(3)}-2F_{00}'' \qquad (4.16)$$

$$\eta F_{01}^{(4)}+2F_{01}^{(3)}=16 \qquad (4.17)$$

Repeat the steps used to solve for F_{00} in the leading order zero equation (4.12) to develop the solution to the leading order first equation from (4.11),

$$F_{01}=\frac{4}{3}\eta^3+c_1+\eta c_2+\eta^2c_3+c_4\left(\eta-\eta\ln(\eta)\right) \qquad (4.18)$$

$$F_{01}(0)=0\rightarrow c_1=0\rightarrow F_{01}=\frac{4}{3}\eta^3+\eta c_2+\eta^2c_3+c_4\left(\eta-\eta\ln(\eta)\right)$$

$$\lim_{\eta\rightarrow0}\left(F_{01}''\sqrt{2\eta}\right)=\sqrt{2\eta}\left(2c_3-\frac{c_4}{\eta}+8\eta\right)=0\rightarrow c_4=0\rightarrow F_{01}=\frac{4}{3}\eta^3+\eta c_2+\eta^2c_3$$

$$F_{01}'\left(\tfrac{1}{2}\right)=1+c_2+c_3=0$$

$$F_{01}\left(\tfrac{1}{2}\right)=1\rightarrow\frac{1}{6}+\frac{c_2}{2}+\frac{c_3}{4}=1\rightarrow c_3=-\frac{4}{3}\ \&\ c_2=\frac{1}{3}$$

$$\boxed{F_{01}=\frac{1}{3}\eta-\frac{4}{3}\eta^2+\frac{4}{3}\eta^3} \qquad (4.19)$$

Substituting equations (4.15) and (4.19) into equation (4.9), the leading order solution is found:

Leading Order Solution: $$\boxed{F_0 = \left(4¦ - 4¦^{2}\right) + \sim\left(\frac{1}{3}¦ - \frac{4}{3}¦^{2} + \frac{4}{3}¦^{3}\right)} \tag{4.20}$$

C. First Order Solution

To solve for F_1 in the first order equation, repeat the steps used to find the leading order solution. The leading order equation is taken from (4.7):

$$\underbrace{¦ F_1^{(4)} + \sim ¦ F_1^{(3)} + \sim 2F_1'' + \frac{1}{2}F_0\, F_0^{(3)} - \frac{1}{2}F_0'\, F_0'' + 2F_1^{(3)}}_{\text{First Order}} = 0 \tag{4.21}$$

Separate the terms and use (4.21) to substitute in for the F_0 terms:

$$¦ F_1^{(4)} + \sim ¦ F_1^{(3)} + \sim 2F_1'' + 2F_1^{(3)} = -\frac{1}{2}F_0\, F_0^{(3)} + \frac{1}{2}F_0'\, F_0'' \tag{4.22}$$

$$F_1 = F_{10} + \sim F_{11} + \ldots \tag{4.23}$$

$$\begin{aligned} &¦ F_{10}^{(4)} + \sim ¦ F_{11}^{(4)} + \sim ¦ F_{10}^{(3)} + \sim^{2} ¦ F_{11}^{(3)} + \sim 2F_{10}'' + \sim^{2} 2F_{11}'' + 2F_{10}^{(3)} + \sim 2F_{11}^{(3)} \\ &= -\frac{1}{2}\left[\left(4¦ - 4¦^{2}\right) + \sim\left(\frac{1}{3}¦ - \frac{4}{3}¦^{2} + \frac{4}{3}¦^{3}\right)\right] 8\sim \\ &+ \frac{1}{2}\left[\left(4 - 8¦\right) + \sim\left(\frac{1}{3} - \frac{8}{3}¦ + 4¦^{2}\right)\right]\left[-8 + \sim\left(-\frac{8}{3} + 8¦\right)\right] \end{aligned} \tag{4.24}$$

$$\begin{aligned} &\underbrace{\left(¦ F_{10}^{(4)} + 2F_{10}^{(3)}\right)}_{\substack{\text{First Order} \\ \text{Zero Equation}}} + \sim \underbrace{\left(¦ F_{11}^{(4)} + ¦ F_{10}^{(3)} + 2F_{10}'' + 2F_{11}^{(3)}\right)}_{\substack{\text{First Order} \\ \text{First Equation}}} \\ &= \underbrace{-16 + 32¦}_{\substack{\text{First Order} \\ \text{Zero Equation}}} + \sim \underbrace{\left(-32¦^{2} + \frac{64}{3}¦ - \frac{20}{3}\right)}_{\substack{\text{First Order} \\ \text{First Equation}}} \end{aligned} \tag{4.25}$$

i. First Order Zero Equation

Solve the linear ordinary differential equation (first order zero equation), and apply the boundary conditions given in (4.2):

$$¦\, F_{10}^{(4)} + 2F_{10}^{(3)} = -16 + 32¦ \tag{4.26}$$

$$F_{10} = -\frac{4}{3}¦^{3} + \frac{4}{9}¦^{4} + c_1 + ¦\, c_2 + ¦^{2} c_3 + c_4\left(¦ - ¦\,\ln(¦)\right) \tag{4.27}$$

$$F_{10}(0) = 0 \rightarrow c_1 = 0 \rightarrow F_{10} = -\frac{4}{3}¦^{3} + \frac{4}{9}¦^{4} + ¦\, c_2 + ¦^{2} c_3 + c_4\left(¦ - ¦\,\ln(¦)\right)$$

$$\lim_{¦ \to 0}\left(F_{10}''\sqrt{2¦}\right) =$$
$$\sqrt{2}\left(2c_3\sqrt{¦} - \frac{c_4}{\sqrt{¦}} - 8¦\sqrt{¦} + \frac{16¦^{2}\sqrt{¦}}{3}\right) = 0 \rightarrow c_4 = 0$$

$$F_{10} = -\frac{4}{3}¦^{3} + \frac{4}{9}¦^{4} + ¦\, c_2 + ¦^{2} c_3$$

$$F_{10}'\left(\tfrac{1}{2}\right) = -\frac{7}{9} + c_2 + c_3 = 0$$

$$F_{10}\left(\tfrac{1}{2}\right) = 1 \rightarrow -\frac{5}{36} + \frac{c_2}{2} + \frac{c_3}{4} = 1 \rightarrow c_3 = 1,\ c_2 = \frac{2}{9}$$

$$\boxed{F_{10} = \frac{4}{9}¦^{4} - \frac{4}{3}¦^{3} + ¦^{2} - \frac{2}{9}¦} \tag{4.28}$$

ii. First Order First Equation

Next, the components for the first order first equation from (4.25) are taken and set equal to each other. Then it is reordered to separate the F_{11} and F_{10} terms:

$$¦\, F_{11}^{(4)} + 2F_{11}^{(3)} = -¦\, F_{10}^{(3)} - 2F_{10}'' - 32¦^{2} + \frac{64}{3}¦ - \frac{20}{3} \tag{4.29}$$

Before substituting the F_{10} terms into (4.29), the derivative forms of (4.28) are determined:

$$F'_{10} = \frac{16}{9}¦^3 - 4¦^2 + 2¦ - \frac{2}{9} \tag{4.30}$$

$$F''_{10} = \frac{16}{3}¦^2 - 8¦ + 2 \tag{4.31}$$

$$F'''_{10} = \frac{32}{3}¦ - 8 \tag{4.32}$$

$$¦ F_{11}^{(4)} + 2F_{11}^{(3)} = -¦\left(\frac{32}{3}¦ - 8\right) - 2\left(\frac{16}{3}¦^2 - 8¦ + 2\right) - 32¦^2 + \frac{64}{3}¦ - \frac{20}{3} \tag{4.33}$$

$$¦ F_{11}^{(4)} + 2F_{11}^{(3)} = -\frac{160}{3}¦^2 + \frac{136}{3}¦ - \frac{32}{3} \tag{4.34}$$

$$F_{11} = -\frac{2}{9}¦^5 + \frac{17}{27}¦^4 - \frac{8}{9}¦^3 + c_1 + ¦ c_2 + ¦^2 c_3 + c_4\left(¦ - ¦ \ln(¦)\right) \tag{4.35}$$

$$F_{11}(0) = 0 \rightarrow c_1 = 0$$

$$F_{11} = -\frac{2}{9}¦^5 + \frac{17}{27}¦^4 - \frac{8}{9}¦^3 + ¦ c_2 + ¦^2 c_3 + c_4\left(¦ - ¦ \ln(¦)\right) \tag{4.36}$$

$$\lim_{¦ \to 0}\left(F''_{11}\sqrt{2¦}\right) = \lim_{¦ \to 0}\left[\sqrt{2¦}\left(2c_3 - \frac{c_4}{¦} - \frac{16¦}{3} + \frac{68¦^2}{9} - \frac{40¦^3}{9}\right)\right] = 0 \rightarrow c_4 = 0$$

$$F_{11} = -\frac{2}{9}¦^5 + \frac{17}{27}¦^4 - \frac{8}{9}¦^3 + ¦ c_2 + ¦^2 c_3 \tag{4.37}$$

$$F'_{11}\left(\tfrac{1}{2}\right) = -\frac{91}{216} + c_2 + c_3 = 0 \rightarrow c_3 = \frac{91}{216} - c_2$$

$$F_{11}\left(\tfrac{1}{2}\right)=1 \rightarrow = \frac{17}{216}+\frac{c_2}{2}+\frac{1}{4}\left(\frac{91}{216}-c_2\right)=1$$

$$\rightarrow c_3=\frac{19}{36} \,\&\, c_2=-\frac{23}{216}$$

$$\boxed{F_{11}=-\frac{2}{9}¦^5+\frac{17}{27}¦^4-\frac{8}{9}¦^3+\frac{19}{36}¦^2-\frac{23}{216}¦} \tag{4.38}$$

Substituting equations (4.28) and (4.38) into equation (4.23), the first order first equation solution becomes

$$\boxed{F_1=\left(\frac{4}{9}¦^4-\frac{4}{3}¦^3+¦^2-\frac{2}{9}¦\right)+\sim\left(-\frac{2}{9}¦^5+\frac{17}{27}¦^4-\frac{8}{9}¦^3+\frac{19}{36}¦^2-\frac{23}{216}¦\right)}. \tag{4.39}$$

D. Complete Solution

Substituting the results from the previous calculations, equations (4.20) and (4.39), into equation (4.4), the solution for F is obtained.

$$\boxed{\begin{aligned}F(¦)=&\left(4¦-4¦^2\right)+\sim\left(\frac{1}{3}¦-\frac{4}{3}¦^2+\frac{4}{3}¦^3\right)+\\ &£\left[\left(\frac{4}{9}¦^4-\frac{4}{3}¦^3+¦^2-\frac{2}{9}¦\right)+\sim\left(-\frac{2}{9}¦^5+\frac{17}{27}¦^4-\frac{8}{9}¦^3+\frac{19}{36}¦^2-\frac{23}{216}¦\right)\right]\end{aligned}} \tag{4.40}$$

Finally, by calculating the derivatives of $F(¦)$, the final substitutions can be made into the governing equation, (4.1). The governing equation is restated below one final time:

$$¦F''''+\sim\left(¦F'''+2F''\right)+\frac{1}{2}R\left(FF'''-F'F''\right)+2F'''=0\,.$$

Chapter 5

Results

The results of the Adomian Decomposition Method are plotted in the following pages. In Figure 3 below, it is apparent that the plots agree with the boundary conditions where the value of $F = 0$ for $\eta = 0$ and $F = 1$ for $\eta = \frac{1}{2}$. For this plot, the sample values of $R = 5$ and $\alpha = 1$ are used. The Adomian Decomposition approximations are plotted along with the perturbation and numerical results [64] for comparison.

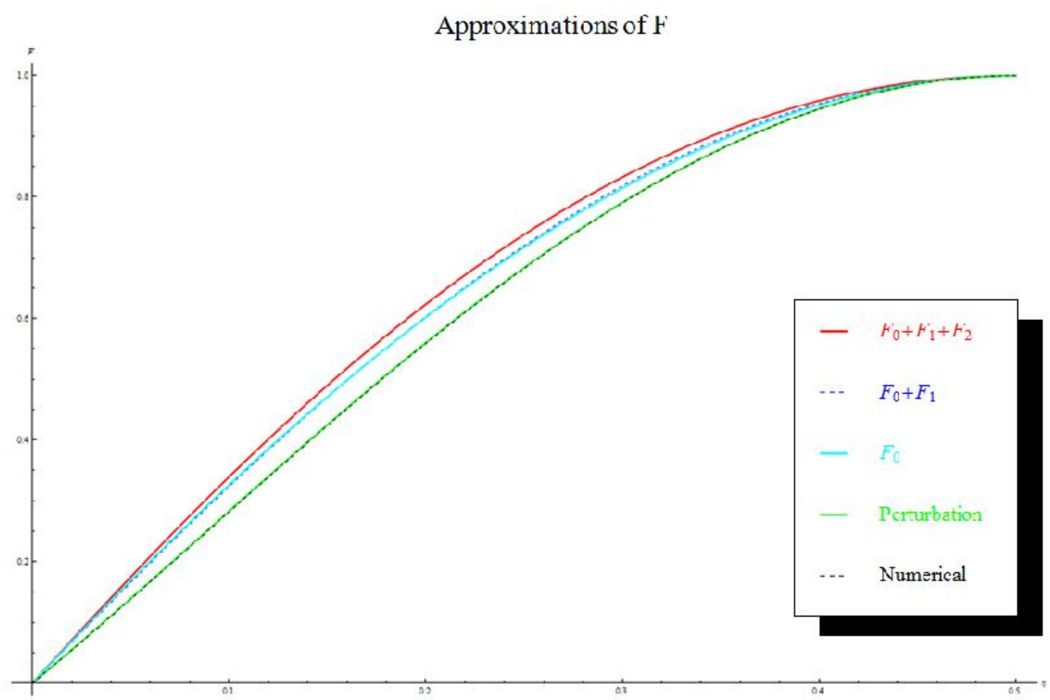

Figure 3. F vs. η for R=5, α=1.

By taking the approximation of F and applying it to the streamfunction (2.9), · , at ¦ $= 0.25$ and using the sample values of ¬ , $R = 1$, and ~ $= 0.5$, the velocity components in the x- and y-directions, u and v, can be calculated. The corresponding velocity field plot is shown in Figure 4.

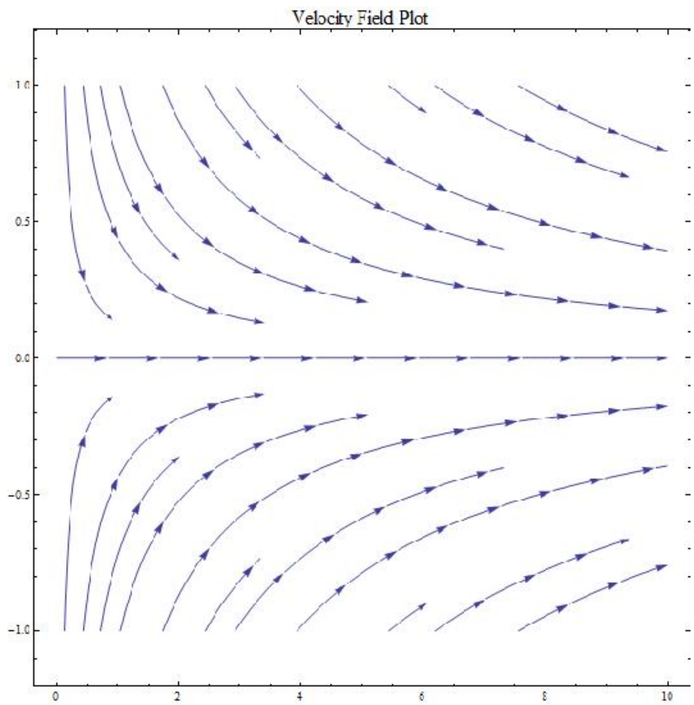

Figure 4. Velocity field plot.

To consider the effects of R, the resulting equation for F versus η is plotted over a range of values in Figure 5, with ~ $= 0.25$. The plot shows that as R exceeds 50, the equation begins to pull much farther away from the plots at smaller R values. As R increases, the value of *F* decreases between the boundary points. Recalling the calculations made in the Adomian Decomposition, R appears at many levels within the zeroth, first, and second order solutions, most often in the denominator. It is, therefore, fitting that changes in R would have significant effects on the resulting solution, as evidenced in Figure 5.

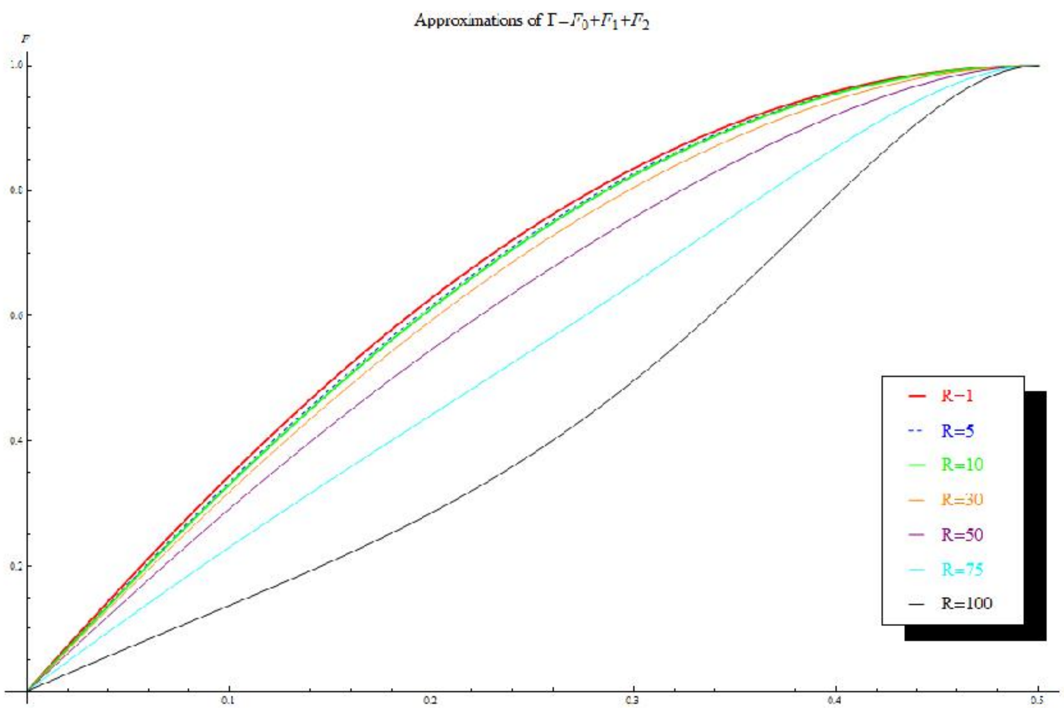

Figure 5. R plots.

To consider the effects of ~ , the result is plotted in Figure 6 over a range of values, while $R = 10$. The figure demonstrates that as ~ increases (closer the value of R), the value of *F* increases between the boundary points. In the calculation steps which solve for F, ~ is commonly found in the numerator, providing for a direct relationship with F.

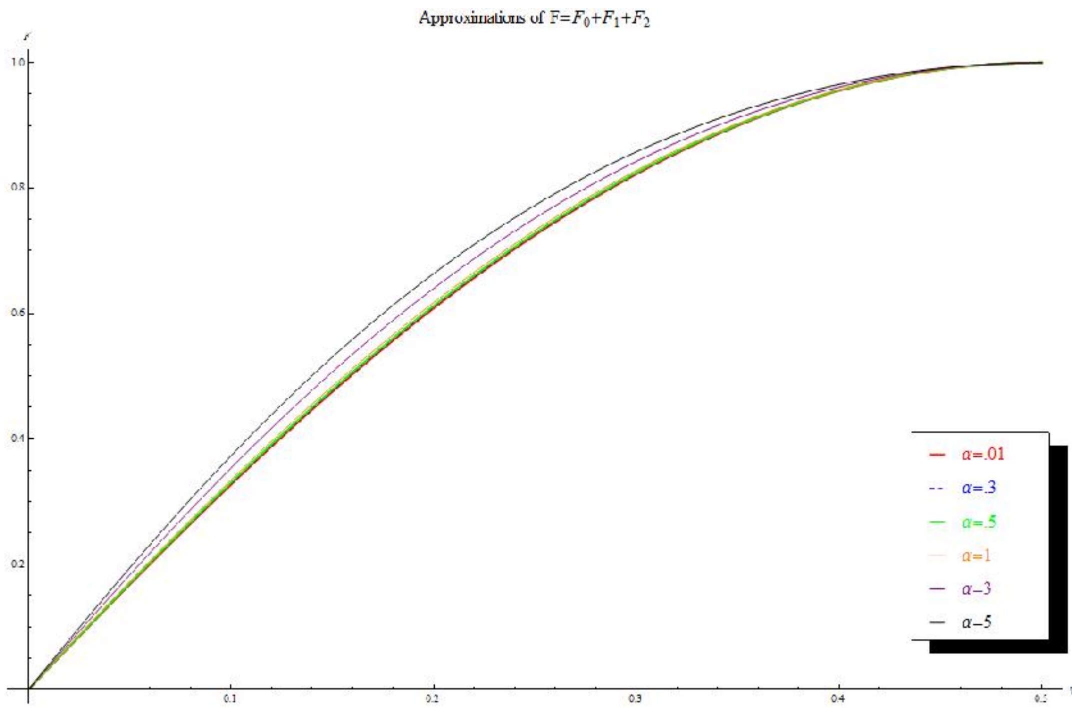

Figure 6. α Plots.

Chapter 6

Conclusion and Future Work

In this study, the Adomian Decomposition Method is used to solve the given flowfield equation. The equation, which can be traced back to research pioneered by Berman [1] in the 1950's, is extended to take into account viscosity, wall regression, and wall permeability. Simplifications to the equation, as a result of disregarding the flame zone and treating the flow as compressible and non-reactive, are included to allow us to derive solutions that are largely in accord with observations.

A. Conclusion

The Adomian Decomposition Method was successfully applied to the governing flowfield equation, which resulted in the approximate solution. The equation was separated into nonlinear, highest-order linear, and the remaining linear terms. The Adomian polynomials were determined, and then the Adomian Decomposition was invoked. Using a four-fold integration as an inverse linear operator, the Adomian polynomials, and the given boundary conditions, the method was applied to obtain the zeroth, first, and second order solutions. These solutions were then added to obtain the final Adomian Decomposition approximate solution, accurate to second order.

B. Future Work

In future work, the Homotopy Analysis Method (HAM) should be applied to the governing equation to provide a solution using another method. Along with the Adomian Decomposition Method and the asymptotic solution, all three methods can also be applied to a different problem, or a different form of the presented problem, to provide researchers with additional insight in their respective theoretical, experimental, and computational research.

List of References

[1] Berman, A. S., “Laminar Flow in Channels with Porous Walls,” *Journal of Applied Physics,* Vol. 24, No. 9, 1953, pp. 1232-1235. doi: 10.1063/1.1721476

[2] Chedevergne, F., Casalis, G., and Féraille, T., “Biglobal Linear Stability Analysis of the Flow Induced by Wall Injection,” *Physics of Fluids,* Vol. 18, No. 1, 2006, pp. 014103-14. doi: 10.1063/1.2160524

[3] Taylor, G., “Fluid Flow in Regions Bounded by Porous Surfaces,” *Proceedings of the Royal Society of London, Series A,* Vol. 234, No. 1199, 1956, pp. 456-475. doi: 10.1098/rspa.1956.0050

[4] Yuan, S., “Further Investigation of Laminar Flow in Channels with Porous Walls,” *Journal of Applied Physics,* Vol. 27, No. 3, 1956, pp. 267-269. doi: 10.1063/1.1722355

[5] Terrill, R., “Laminar Flow in a Uniformly Porous Channel with Large Injection,” *The Aeronautical Quarterly,* Vol. 16, 1965, pp. 323-332.

[6] Sellars, J., “Laminar Flow in Channels with Porous Walls at High Suction Reynolds Numbers,” *Journal of Applied Physics,* Vol. 26, No. 4, 1955, pp. 489-490. doi: 10.1063/1.1722024

[7] Terrill, R., “Laminar Flow in a Uniformly Porous Channel (Laminar Flow in Two-Dimensional Channel with Porous Walls Assuming Uniformly Injected Fluid),” *The Aeronautical Quarterly,* Vol. 15, 1964, pp. 299-310.

[8] Proudman, I., “An Example of Steady Laminar Flow at Large Reynolds Number,” *Journal of Fluid Mechanics,* Vol. 9, No. 4, 1960, pp. 593-602. doi: 10.1017/S002211206000133X

[9] Shrestha, G., and Terrill, R., “Laminar Flow with Large Injection through Parallel and Uniformly Porous Walls of Different Permeability,” *Quarterly Journal of Mechanics and Applied Mathematics,* Vol. 21, No. 4, 1968, pp. 413-432. doi: 10.1093/qjmam/21.4.413

[10] Morduchow, M., “On Laminar Flow through a Channel or Tube with Injection: Application of Method of Averages,” *Quarterly Journal of Applied Mathematics,* Vol. 14, No. 4, 1957, pp. 361-368.

[11] White Jr., F., Barfield, B., and Goglia, M., “Laminar Flow in a Uniformly Porous Channel,” *Transactions of the American Society of Mechanical Engineers: Journal of Applied Mechanics,* Vol. 25, 1958, pp. 613-617.

[12] Cox, S., “Two-Dimensional Flow of a Viscous Fluid in a Channel with Porous Walls,” *Journal of Fluid Mechanics,* Vol. 227, No. 1, 1991, pp. 1-33. doi: 10.1017/S0022112091000010

[13] King, J., and Cox, S., “Asymptotic Analysis of the Steady-State and Time-Dependent Berman Problem,” *Journal of Engineering Mathematics,* Vol. 39, No. 1, 2001, pp. 87-130. doi: 10.1023/A:1004824527547

[14] Zaturska, M., Drazin, P., and Banks, W., “On the Flow of a Viscous Fluid Driven Along a Channel by Suction at Porous Walls,” *Fluid Dynamics Research,* Vol. 4, No. 3, 1988, pp. 151-178. doi: 10.1016/0169-5983(88)90021-4

[15] Taylor, C., Banks, W., Zaturska, M., and Drazin, P., "Three-Dimensional Flow in a Porous Channel," *Quarterly Journal of Mechanics and Applied Mathematics,* Vol. 44, No. 1, 1991, pp. 105-133. doi: 10.1093/qjmam/44.1.105

[16] Watson, E., Banks, W., Zaturska, M., and Drazin, P., "On Transition to Chaos in Two-Dimensional Channel Flow Symmetrically Driven by Accelerating Walls," *Journal of Fluid Mechanics,* Vol. 212, No. 1, 1990, pp. 451-485. doi: 10.1017/S0022112090002051

[17] Watson, P., Banks, W., Zaturska, M., and Drazin, P., "Laminar Channel Flow Driven by Accelerating Walls," *European Journal of Applied Mathematics,* Vol. 2, No. 4, 1991, pp. 359-385. doi: 10.1017/S0956792500000607

[18] Cox, S., and King, A., "On the Asymptotic Solution of a High-Order Nonlinear Ordinary Differential Equation," *Proceedings of the Royal Society of London, Series A,* Vol. 453, No. 1959, 1997, pp. 711-728. doi: 10.1098/rspa.1997.0040

[19] MacGillivray, A., and Lu, C., "Asymptotic Solution of a Laminar Flow in a Porous Channel with Large Suction: A Nonlinear Turning Point Problem," *Methods and Applications of Analysis,* Vol. 1, No. 2, 1994, pp. 229-248.

[20] Lu, C., "On the Asymptotic Solution of Laminar Channel Flow with Large Suction," *SIAM Journal on Mathematical Analysis,* Vol. 28, No. 5, 1997, pp. 1113-1134. doi: 10.1137/S0036141096297704

[21] Varapaev, V., and Yagodkin, V., "Flow Stability in a Channel with Porous Walls," *Fluid Dynamics (Izvestiya Akademii Nauk SSSR, Meckanika Zhidkosti i Gaza),* Vol. 4, No. 5, 1969, pp. 91-95. doi: 10.1007/BF01015958

[22] Raithby, G., and Knudsen, D., "Hydrodynamic Development in a Duct with Suction and Blowing," *Journal of Applied Mechanics,* Vol. 41, 1974, pp. 896-902.

[23] Hocking, L., "Non-Linear Instability of the Asymptotic Suction Velocity Profile," *Quarterly Journal of Mechanics and Applied Mathematics,* Vol. 28, No. 3, 1975, pp. 341-353. doi: 10.1093/qjmam/28.3.341

[24] Sviridenkov, A., and Yagodkin, V., "Flows in the Initial Sections of Channels with Permeable Walls," *Fluid Dynamics (Izvestiya Akademii Nauk SSSR, Meckanika Zhidkosti i Gaza),* Vol. 11, No. 5, 1976, pp. 689-693. doi: 10.1007/BF01012958

[25] Brady, J. F., "Flow Development in a Porous Channel or Tube," *Physics of Fluids,* Vol. 27, No. 5, 1984, pp. 1061-1067. doi: 10.1063/1.864735

[26] Durlofsky, L., and Brady, J., "The Spatial Stability of a Class of Similarity Solutions," *Physics of Fluids,* Vol. 27, No. 5, 1984, pp. 1068-1076. doi: 10.1063/1.864736

[27] Robinson, W., "The Existence of Multiple Solutions for the Laminar Flow in a Uniformly Porous Channel with Suction at Both Walls," *Journal of Engineering Mathematics,* Vol. 10, No. 1, 1976, pp. 23-40. doi: 10.1007/BF01535424

[28] Skalak, F., and Wang, C., "On the Nonunique Solutions of Laminar Flow through a Porous Tube or Channel," *SIAM Journal on Applied Mathematics,* Vol. 34, No. 3, 1978, pp. 535-544. doi: 10.1137/0134042

[29] Shih, K., “On the Existence of Solutions of an Equation Arising in the Theory of Laminar Flow in a Uniformly Porous Channel with Injection,” *SIAM Journal on Applied Mathematics,* Vol. 47, No. 3, 1987, pp. 526-533. doi: 10.1137/0147035

[30] Hastings, S., Lu, C., and MacGillivray, A., “A Boundary Value Problem with Multiple Solutions from the Theory of Laminar Flow,” *SIAM Journal on Mathematical Analysis,* Vol. 23, No. 1, 1992, pp. 201-208. doi: 10.1137/0523010

[31] Lu, C., MacGillivray, A., and Hastings, S., “Asymptotic Behaviour of Solutions of a Similarity Equation for Laminar Flows in Channels with Porous Walls,” *IMA Journal of Applied Mathematics,* Vol. 49, No. 2, 1992, pp. 139-162. doi: 10.1093/imamat/49.2.139

[32] Casalis, G., Avalon, G., and Pineau, J.-P., “Spatial Instability of Planar Channel Flow with Fluid Injection through Porous Walls,” *Physics of Fluids,* Vol. 10, No. 10, 1998, pp. 2558-2568. doi: 10.1063/1.869770

[33] Saad, T., and Majdalani, J., “Rotational Flowfields in Porous Channels with Arbitrary Headwall Injection,” *Journal of Propulsion and Power,* Vol. 25, No. 4, 2009, pp. 921-929. doi: 10.2514/1.41926

[34] Kurdyumov, V. N., “Viscous and Inviscid Flows Generated by Wall-Normal Injection into a Cylindrical Cavity with a Headwall,” *Physics of Fluids,* Vol. 20, No. 12, 2008, pp. 123602-7. doi: 10.1063/1.3045738

[35] Chu, W., Yang, V., and Majdalani, J., “Premixed Flame Response to Acoustic Waves in a Porous-Walled Chamber with Surface Mass Injection,” *Combustion and Flame,* Vol. 133, No. 3, 2003, pp. 359-370. doi: 10.1016/S0010-2180(03)00018-X

[36] Vyas, A., Majdalani, J., and Yang, V., “Estimation of the Laminar Premixed Flame Temperature and Velocity in Injection-Driven Combustion Chambers,” *Combustion and Flame,* Vol. 133, No. 3, 2003, pp. 371-374. doi: 10.1016/S0010-2180(03)00017-8

[37] Apte, S., and Yang, V., “Effect of Acoustic Oscillation on Flow Development in a Simulated Nozzleless Rocket Motor,” *Solid Propellant Chemistry, Combustion, and Motor Interior Ballistics,* Vol. 185, edited by V. Yang, T. B. Brill, and W.-Z. Ren, AIAA Progress in Astronautics and Aeronautics, Washington, DC, 2000, pp. 791-822.

[38] Lee, Y., and Beddini, R. A., “Acoustically-Induced Turbulent Transition in Solid Propellant Rocket Chamber Flowfields,” AIAA Paper 99-2508, June 1999.

[39] Lee, Y., and Beddini, R. A., “Effect of Solid Rocket Chamber Pressure on Acoustically-Induced Turbulent Transition,” AIAA Paper 2000-3802, July 2000.

[40] Majdalani, J., “Multiple Asymptotic Solutions for Axially Travelling Waves in Porous Channels,” *Journal of Fluid Mechanics,* Vol. 636, No. 1, 2009, pp. 59-89. doi: 10.1017/S0022112009007939

[41] Majdalani, J., and Roh, T., “The Oscillatory Channel Flow with Large Wall Injection,” *Proceedings of the Royal Society of London, Series A,* Vol. 456, No. 1999, 2000, pp. 1625-1657. doi: 10.1098/rspa.2000.0579

[42] Jackson, T. L., Buckmaster, J., Campbell, M., Kochevets, S., and Massa, L., "The Burning of 3-D Random-Pack Heterogeneous Propellants," AIAA Paper 2001-3952, July 2001.

[43] Buckmaster, J., Jackson, T. L., and Ulrich, M., "Numerical Modeling of Heterogeneous Propellant Combustion," AIAA Paper 2001-3579, July 2001.

[44] Tsangaris, S., and Leiter, E., "On Laminar Steady Flow in Sinusoidal Channels," *Journal of Engineering Mathematics,* Vol. 18, No. 2, 1984, pp. 89-103. doi: 10.1007/BF00042729

[45] Barron, J., Majdalani, J., and Van Moorhem, W. K., "A Novel Investigation of the Oscillatory Field over a Transpiring Surface," *Journal of Sound and Vibration,* Vol. 235, No. 2, 2000, pp. 281-297. doi: 10.1006/jsvi.2000.2920

[46] Ma, Y., Van Moorhem, W., and Shorthill, R., "Experimental Investigation of Velocity Coupling in Combustion Instability," *Journal of Propulsion and Power,* Vol. 7, No. 5, 1991, pp. 692-699. doi: 10.2514/3.23381

[47] Ma, Y., Van Moorhem, W., and Shorthill, R., "Innovative Method of Investigating the Role of Turbulence in the Velocity Coupling Phenomenon," *Journal of Vibration and Acoustics-Transactions of the ASME,* Vol. 112, No. 4, 1990, pp. 550-555. doi: 10.1115/1.2930141

[48] Uchida, S., and Aoki, H., "Unsteady Flows in a Semi-Infinite Contracting or Expanding Pipe," *Journal of Fluid Mechanics,* Vol. 82, No. 2, 1977, pp. 371-387. doi: 10.1017/S0022112077000718

[49] Goto, M., and Uchida, S., "Unsteady Flows in a Semi-Infinite Expanding Pipe with Injection through Wall," *Transactions of the Japan Society for Aeronautical and Space Sciences,* Vol. 33, No. 9, 1990, pp. 14-27.

[50] Kozinski, A., Schmidt, F., and Lightfoot, E., "Velocity Profiles in a Porous-Walled Duct," *Industrial and Engineering Chemical Fundamentals,* Vol. 9, No. 3, 1970, pp. 502-505. doi: 10.1021/i160035a033

[51] Wang, C., "Pulsatile Flow in a Porous Channel," *Journal of Applied Mechanics,* Vol. 38, No. 2, 1971, pp. 553-555. doi: 10.1115/1.3408822

[52] Bhatnagar, R. K., "Fluctuating Flow of a Viscoelastic Fluid in a Porous Channel," *Journal of Applied Mechanics*, Vol. 46, No. 1, 1979, pp. 21-25.

[53] Traineau, J. C., Hervat, P., and Kuentzmann, P., "Cold-Flow Simulation of a Two-Dimensional Nozzleless Solid-Rocket Motor," AIAA Paper 86-1447, July 1986.

[54] Avalon, G., Casalis, G., and Griffond, J., "Flow Instabilities and Acoustic Resonance of Channels with Wall Injection," AIAA Paper 98-3218, July 1998.

[55] Griffond, J., and Casalis, G., "On the Dependence on the Formulation of Some Nonparallel Stability Approaches Applied to the Taylor Flow," *Physics of Fluids,* Vol. 12, No. 2, 2000, pp. 466-468. doi: 10.1063/1.870323

[56] Griffond, J., and Casalis, G., "On the Nonparallel Stability of the Injection Induced Two-Dimensional Taylor Flow," *Physics of Fluids,* Vol. 13, No. 6, 2001, pp. 1635-1644. doi: 10.1063/1.1367869

[57] Apte, S., and Yang, V., “Effects of Acoustic Oscillations on Turbulent Flowfield in a Porous Chamber with Surface Transpiration,” AIAA Paper 98-3219, July 1998.
[58] Liou, T., and Lien, W., “Numerical Simulations of Injection-Driven Flows in a Two-Dimensional Nozzleless Solid-Rocket Motor,” *Journal of Propulsion and Power*, Vol. 11, No. 4, 1995, pp. 600-606. doi: 10.2514/3.23886
[59] Liou, T., Lien, W., and Hwang, P., “Transition Characteristics of Flowfield in a Simulated Solid-Rocket Motor,” *Journal of Propulsion and Power,* Vol. 14, No. 3, 1998, pp. 282-289. doi: 10.2514/2.5295
[60] Dauenhauer, E., and Majdalani, J., “Exact Self-Similarity Solution of the Navier-Stokes Equations for a Porous Channel with Orthogonally Moving Walls,” *Physics of Fluids*, Vol. 15, No. 6, 2003, pp. 1485-1495. doi: 10.1063/1.1567719
[61] White, F. M., *Viscous Fluid Flow*, McGraw-Hill, New York, 1991.
[62] Majdalani, J., Vyas, A., and Flandro, G., “Erratum on Higher Mean-Flow Approximation for a Solid Rocket Motor with Radially Regressing Walls,” *AIAA Journal*, Vol. 47, No. 1, 2009, pp. 286-286. doi: 10.2514/1.40061
[63] Majdalani, J., Vyas, A., and Flandro, G., “Higher Mean-Flow Approximation for a Solid Rocket Motor with Radially Regressing Walls,” *AIAA Journal*, Vol. 40, No. 9, 2002, pp. 1780-1788. doi: 10.2514/2.1854
[64] Saad, Tony. *Flow in Porous Pipe with Regressing Walls*. Computer software. N.p., n.d. Web. 6 Aug. 2014.

Vita

Jeisson J. Parra graduated from Embry-Riddle Aeronautical University, Daytona Beach, Florida in May 2008. He received a B.S. in Aerospace Engineering, with a concentration in Astronautics and a minor in Mathematics. In August 2008, he joined UTSI as a Graduate Research Assistant working under Dr. Majdalani. In August 2010, he left UTSI to accept a position as an Aero-Mechanical Engineer in the defense contracting industry. Later, he moved on to a position as an Aerospace Design Engineer in the gas turbine industry, where he continues to work at the time of this writing. He will graduate in December 2014 with a Master of Science in Aerospace Engineering.